# MATHEMATICAL MODELS IN POPULATION DYNAMICS

BY
ALEXANDER SALISBURY

A Thesis

Submitted to the Division of Natural Sciences
New College of Florida
in partial fulfillment of the requirements for the degree
Bachelor of Arts
Under the sponsorship of Dr. Necmettin Yildirim

Sarasota, FL
April, 2011

# ACKNOWLEDGEMENTS

I would like to thank my advisor Dr. Necmettin Yildirim for his support, guidance, and seemingly unlimited supply of patience. Additional thanks to my thesis committee members Dr. Chris Hart and Dr. Eirini Poimenidou for their guidance and criticism. Final thanks to family and friends for their love and support.

# TABLE OF CONTENTS

# LIST OF TABLES AND FIGURES

# MATHEMATICAL MODELS IN POPULATION DYNAMICS

Alexander Salisbury

New College of Florida, 2011

## ABSTRACT

Population dynamics studies the changes in size and composition of populations through time, as well as the biotic and abiotic factors influencing those changes. For the past few centuries, ordinary differential equations (ODEs) have served well as models of both single-species and multispecies population dynamics.

In this study, we provide a mathematical framework for ODE model analysis and an outline of the historical context surrounding mathematical population modeling. Upon this foundation, we pursue a piecemeal construction of ODE models beginning with the simplest one-dimensional models and working up in complexity into two-dimensional systems. Each modeling step is complimented with mathematical analysis, thereby elucidating the model's behaviors, and allowing for biological interpretations to be established.

Dr. Necmettin Yildirim
Division of Natural Sciences

# CHAPTER 1: BACKGROUND

The aim of this section is to elaborate on basic concepts and terminology underlying the study of dynamical systems. Here, we provide a basic review of the literature to date with the intent of fostering a better understanding of concepts and analyses that are used in later sections. We will begin an introduction to ordinary differential equation (ODE) models and methods of analysis that have been developed over the past several centuries, followed by an historical overview of the "field" of dynamics. Applications in population ecology will be of particular emphasis.

## 1.1 WHAT ARE DYNAMICAL SYSTEMS?

A system may be loosely defined as an assemblage of interacting or interdependent objects that collectively form an integrated "whole." *Dynamical systems* describe the evolution of systems in *time*. A dynamical system is said to have a *state* for every point in time, and the state is subject to an *evolution rule*, which determines what future states may follow from the current, or initial, state. Whether the system settles down to a state of equilibrium, becomes fixed into steadily oscillating cycles, or fluctuates chaotically, it is the system's *dynamics* that describe what is occurring (Strogatz, 1994). A system that appears steady and stable is, in fact, the result of forces acting in cohort to produce a balance of

tendencies. In certain instances, only a small perturbation is required to move the system into a completely different state. This occurrence is called a *bifurcation*.

Systems of naturally occurring phenomena are generally constituted by discrete subsystems with their own sets of internal forces. Thus, in order to avoid problems of intractable complexity, the system must be simplified via the observer's discretion. For instance, we might say that for the microbiologist, the system in question is the cell, and likewise, the organ for the physiologist, the population for the ecologist, and so on. An apt model thus requires a carefully selected set of variables chosen to represent the corresponding real-world phenomenon under investigation.

Detailing complex systems requires a language for precise description, and as it turns out, *mathematical models* serve well to describe the systems under consideration. Dynamical systems may be represented in a variety of ways. They are most commonly represented by continuous ordinary differential equations (ODEs) or discrete difference equations. Other manifestations are frequently found in partial differential equations (PDEs), lattice gas automata (LGA), cellular automata (CA), etc. The focus of this work lies primarily on systems represented through ODEs.

The dynamic behavior of a system may be determined by inputs from the environment, but as is often the case, *feedback* from the system allows it to regulate its own dynamics internally. Feedback loops are characterized as *positive* or *negative*. A typical example of a positive feedback loop is demonstrated by so-called "arms races," whereby two sovereign powers escalate arms production in response to each other, leading to an explosion of uncontrolled output. In contrast, negative feedback is exemplified by the typical household thermostat, whereby perturbations in temperature are regulated by the

thermostat's response, which maintains temperature constancy by either sending a heated or cooled output. Thus, positive feedback tends to amplify perturbations to the system, or amplify the system's initial state, while negative feedback tends to dampen disturbances to the system as time progresses. As we shall see throughout this work, feedback plays an important role in the stability of systems.

A system is said to be at *equilibrium* if opposing forces in the system are balanced, and in turn the state of the system remains constant and unchanged. A system is said to be *stable* if its state returns to a state of equilibrium following some perturbation (e.g., an environmental disturbance). A system is *globally stable* if its state returns to equilibrium following a perturbation of *any* magnitude, whereas, a *locally stable* system indicates that displacements must occur in a defined *neighborhood* of the equilibrium in order for the system to return to the same state of equilibrium.

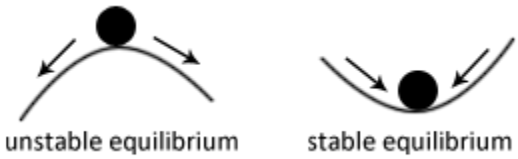


**Figure 1.1.** Rolling-ball analogy for stable and unstable equilibria.

The notion of stability is illustrated in Figure 1.1 by means of a ball resting atop a peak (unstable position) and in the dip of a valley (stable position). Imagining a landscape with multiple peaks and valleys is, by analogy, to imagine a global landscape with multiple local points of stability (valleys) and of instability (peaks). The peaks in the landscape define the *thresholds* separating each of the distinct equilibria, and therefore the level of perturbation that the system must undergo is analogous to that of the peak's magnitude. Systems and their stability are considered in greater depth in Section 1.3.

## 1.2 FORMULATING THE MODEL

When we refer to dynamical systems, in fact, we are generally referring to an abstracted mathematical *model*, as opposed to the actual empirical phenomenon whose dynamics we are attempting to describe. We begin by attempting to identify the physical variables that we believe are responsible for the behavior of the phenomenon in question, and then we may formulate an equation, or system of equations, which also reflects the interrelation of our assumed variables. As depicted in Figure 1.2, the model-building process involves the repetitive steps of observation, deduction, (re)formulation, and validation (Berryman & Kindlmann, 2008).

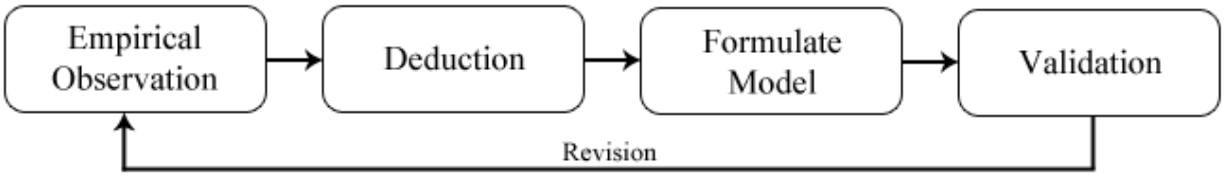


**Figure 1.2.** Flow diagram of general modeling process

A basic aim of modeling is to help illuminate the mechanics that underlie some real-world phenomenon, whether its nature is biological, chemical, physical, economic, or otherwise. Obtaining results that are consistent with the real-world phenomenon is a necessary but not sufficient property of a good model, and as we shall see, there are several criteria by which an apt model should be upheld.

The first step in formulating a model is to delineate the major factors governing the real-world situation that is to be modeled (Berryman & Kindlmann, 2008). Conceptualizing the problem such that all key variables are accounted for, insofar as they reflect the mechanics of the observable phenomenon, is a good method for producing a testable

model. Initial sketches of a model may be done using a flow chart diagram or pseudocode, which illustrates state variables and the nature of their connections.

Gilpin & Ayala (1973) propose the following criteria by which a good model should uphold:

1. *Simplicity.* By virtue of Occam's razor, simple models are favorable over complicated models "because their empirical content is greater; and because they are better testable" (Popper, 1992). Incorporating the minimum possible number of parameters to account for the observed results is always favorable. As Albert Einstein famously stated, "Everything should be made as simple as possible, but not simpler."
2. *Reality.* All of the model's parameters should have biological relevance and attempt to reflect the mechanics of the biological system in question. The modeler should therefore hold a sound understanding of the real-world phenomenon in question.

   Models that *explain* a phenomenon from 'first principles' or from the bottom-up are said to be *mechanistic.* They acknowledge that a biological phenomenon is the sum of multiple distinct, yet intertwined, processes, and therefore they attempt to describe the phenomenon in terms of its primary mechanisms (in ecology, often at the level of the *individual*).

   By contrast, models that *describe* a phenomenon are said to be *phenomenological*. The structure of a phenomenological model is empirically determined top-down from a population's characteristics, and therefore cannot predict behaviors independent of the original data. The parameters used in phenomenological models are therefore conglomerate sums of numerous lower-level mechanisms; (Schoener) calls them "megaparameters" (1986).

Schoener provides a worthwhile summary of the mechanistic approach in ecological modeling (1986), ultimately favoring it over the phenomenological approach by imagining a "mechanistic ecologist's utopia." However, both modeling approaches, mechanistic and phenomenological, have their advantages and disadvantages in different scenarios. Nearly all of the models we have chosen to consider herein are phenomenological because they offer a comparatively convenient mathematical form and flexibility in terms of analysis.

3. *Generality*. Using dimensionless variables allows magnitudes to take on a general significance, in turn providing scalability. Then, for specific scenarios the general model may take on specificity to account for the particular case.
4. *Accuracy*. The model should vary from the observed data as little as possible. Hence a model with little to no predictive or explanatory utility should undergo further revision.

Prior to embarking on the step-by-step procedures used to formulate and analyze continuous population models, we will consider population dynamics modeling from an historical perspective, providing insights into the key figures associated with the field of population ecology in addition to the methods they developed in order to understand population systems from a mathematical perspective. Additionally, we shall take this as an opportunity to introduce new terms and concepts.

## 1.3 METHODS FOR ANALYSIS OF POPULATION DYNAMICS

There are multiple techniques employed for interpreting the behaviors of population dynamics models. However, not all continuous models may be analyzed using the same toolset, and in many cases explicit solutions are impossible to achieve. We will be primarily considering two complimentary techniques of analysis: algebraic and geometric, which provide information regarding equilibria and their stability. All of the models we consider are based on ordinary differential equations, and thus, any person with a background in calculus should be capable of understanding the techniques covered.

### *Solving Differential Equations*

Most continuous models of population dynamics are based on differential equations, which can be solved using a variety of techniques, which will in large part be omitted from this study. Unfortunately, only the simplest of models are analytically solvable, leaving the necessity for other techniques of analysis for models with greater complexity. Examples of equations solved in a step-by-step fashion are in Chapter 2.

In light of the fact that some models are too difficult to solve, or are simply unsolvable (e.g, multispecies models discussed in Chapter 3), additional methods must be used in order to gain knowledge about the system's behaviors.

### *Expressing in Dimensionless Form*

Several advantages are conferred by expressing a model in *dimensionless* or *nondimensional* terms. First, the units of measure are not important in calculations and in any case may be brought back into the model at the end of analysis. Recalling from Section 1.2, the criteria for *simplicity* and *generality*; these features are upheld by expressing the

model in dimensionless terms without fear of any loss of generality. More importantly, reducing the number of relevant parameters into dimensionless groupings better illuminates the relationships between parameters, while simultaneously allowing calculations to be made with greater ease.

For example, consider Verhulst's logistic equation, which has a net growth rate parameter $r > 0$ and a carrying capacity parameter $K > 0$.

$$\frac{dN}{dt} = rN\left(1 - \frac{N}{K}\right), \quad N(0) = N_0. \tag{1.1}$$

Here, we may introduce population and time in terms of dimensionless quantities, respectively, by

$$Q = \frac{N}{K}, \text{ and } \tau = rt. \tag{1.2}$$

Rewriting the equation in the dimensionless terms, we obtain

$$\begin{aligned} \frac{dN}{dt} &= \frac{dN}{dQ}\frac{dQ}{d\tau}\frac{d\tau}{dt} \\ &= K\frac{dQ}{d\tau}r \\ &= rKQ(1-Q), \end{aligned} \tag{1.3}$$

Solving for Eq. (1.3) for $\frac{dQ}{d\tau}$ and putting Eq. (1.1) back in, we get

$$\frac{dQ}{d\tau} = Q(1-Q), \; Q(0) = Q_0 \tag{1.4}$$

where $Q_0 = N_0 / K$ is dimensionless. From this point, there are no parameters except $Q_0$, and the model can be solved using standard methods.

***One-Dimensional Models: Geometrical Analysis***

Qualitatively-informed geometrical analysis of differential equations provides a visual representation of the system's dynamics, allowing one to gain a general insight into the behaviors of the system without the need to solve or compute. Determining a system's stability is an important yet easily-achieved process for one-dimensional systems. Here we may recall the concepts of *local* versus *global* stability that were introduced in Section 1.1, but first let us define *stability* more precisely.

Consider the following one-dimensional differential equation:

$$\frac{dN}{dt} = f(N), \tag{1.5}$$

where $f(N)$ is a continuously differentiable (typically nonlinear) function of $N$. We say that $N = N^*$ is an *equilibrium point* (also known as a *fixed point*, *steady state*, *critical point*, or *rest point*) where $\frac{dN}{dt}\Big|_{N=N^*} = 0$. Equilibrium points can be calculated by solving $f(N^*) = 0$. That is to say, at equilibrium, there are no changes occurring in the system through time. It should be noted that there could be more than one value of $N^*$ that satisfies $f(N^*) = 0$. For instance, in addition to whatever equilibrium points a population $N$ may reach (where $N^* > 0$), a *trivial* equilibrium generally found where $N^* = 0,$ indicating the biologically non-trivial fact that a population may not grow from a population of zero individuals. We can also note that if $f(N) > 0,$ then $N$ will increase, and if $f(N) < 0,$ then $N$ will decrease.

By plotting the *phase line* of $\frac{dN}{dt}$ as a function of $N$, it becomes an easy task to gain insight into the system's dynamics. Simply, the points of intersection at the *N*-axis indicate that they are fixed-points since $f(N^*) = 0$ at those points.

Equilibrium points are classified as either *stable* or *unstable*. In Figure 1.3, stable equilibrium points are represented graphically as filled-in dots, and in stable equilibria perturbations dampen over time. By contrast, unstable equilibrium points are represented as unfilled dots, and in unstable equilibria disturbances grow in time. Unstable equilibrium points also may be referred to as *sources* or *repellers*, and stable equilibrium points may be referred to as *sinks* or *attractors*.

An equilibrium point $N^*$ is *asymptotically stable* if all (sufficiently small) perturbations produce only small deviations that eventually return to the equilibrium. Suppose that $N^*$ is a fixed-point and that $f(N)$ is a continuously differentiable function, and $f'(N^*) \neq 0$. Then the fixed-point $N^*$ is considered asymptotically stable if $f'(N^*) < 0$, and asymptotically unstable if $f'(N^*) > 0$.

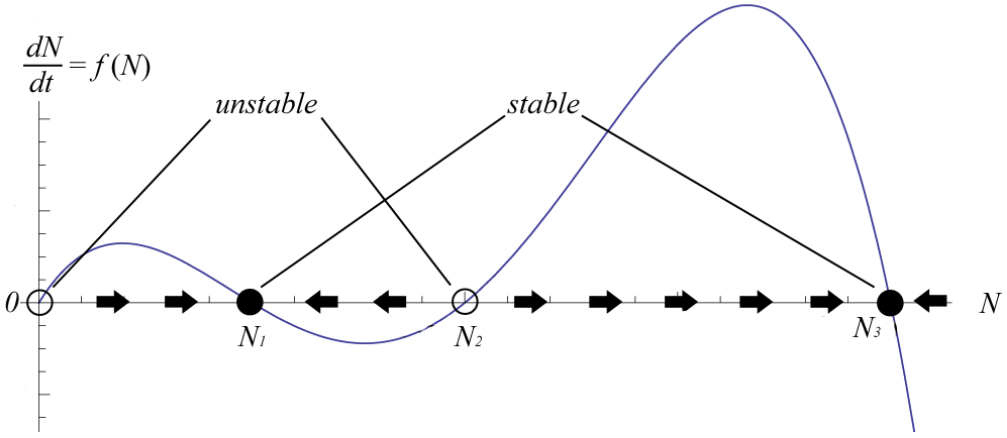


**Figure 1.3.** Phase line portrait of a population model $\frac{dN}{dt} = f(N)$. The trajectory has 3 non-trivial equilibria $N_1, N_2, N_3$.

***One-Dimensional Models: Local Linearization***

The aforementioned geometrical techniques serve a utility by providing a means of intuitive analysis of equilibrium points that is *qualitative* in nature. A complimentary form

of steady state (equilibrium) analysis is achieved by linearizing the equation locally about the equilibrium points. For this section, we will be following along the lines of (Kaplan & Glass, 1995).

Reconsider Eq. (1.5):

$$\frac{dN}{dt} = f(N).$$

We may recall that the equation's equilibrium points are found by solving $f(N) = 0$ for $N$, and such values of $N$ are denoted $N^*$.

Performing a Taylor series expansion of $f(N)$ for each equilibrium point $N^*$ in its neighborhood yields

$$f(N) = f(N^*) + \left.\frac{df}{dN}\right|_{N=N^*}(N - N^*) + \frac{1}{2}\left.\frac{d^2 f}{dN^2}\right|_{N=N^*}(N - N^*)^2 + \cdots. \tag{1.6}$$

In the neighborhood (i.e., within very close proximity) of $N^*$, all higher order terms such as $(N - N^*)^2$ are insignificant compared to $(N - N^*)$, and therefore they are removed from the equation and $f(N^*) = 0$, yielding an approximated form of $f(N)$ given by the function

$$f(N) = \left.\frac{df}{dN}\right|_{N=N^*}(N - N^*).$$

We may further simplify by defining two new variables $m = \left.\frac{df}{dN}\right|_{N=N^*}$ and $x = N - N^*$, which gives $\frac{dx}{dt} = \frac{d}{dt}(N - N^*) = \frac{dN}{dt}$. Therefore Eq. (1.6) becomes

$$f(N) = \frac{dx}{dt} = mx. \tag{1.7}$$

This result is the linear equation for exponential growth or decay (described in further depth in Chapter 2). Thus, if $m > 0$ then there is an exponential departure from the fixed

point, indicating that it is *unstable*. By contrast, if $m < 0$, then there will be an exponential convergence to the equilibrium point, indicating that it is *stable*.

### *Two-Dimensional Models: Geometrical Analysis*

Prior qualitative analysis was limited to one-dimensional models; here we will extend the case to include two-dimensional systems.

Consider the following two-dimensional system of equations:

$$\frac{dN_1}{dt} = f(N_1, N_2), \tag{1.8}$$

$$\frac{dN_2}{dt} = g(N_1, N_2). \tag{1.9}$$

The *phase plane* is the two-dimensional phase space on which the system's trajectories are mapped, thus allowing certain behaviors to be visualized geometrically, and without the necessity for an analytic solution. The *vector field*, or *slope field*, of Eqs. (1.8) and (1.9) is plotted by choosing any arbitrary point $(\overset{0}{N}_1, \overset{0}{N}_2)$ in the plane and substituting the point for $(N_1, N_2)$ in the equations to obtain the slope at that point. Repeating this process at arbitrary but consistent intervals across the plane, while plotting each slope as a *line segment*, achieves an approximate view of where the system's *integral curves* lie. These are unique parametric curves that lie tangent to the line segments.

Finding the *nullclines*, or *zero-growth isoclines*, of the system provides additional information on the system's dynamics. An isocline occurs where line segments in the vector field all have the same slope. Nullclines are a special case of isocline where the slope equals zero; thus, the $N_1$-nullcline is found when $f(N_1, N_2) = 0$ and the $N_2$-nullcline is found when $g(N_1, N_2) = 0$. Their point of intersection marks the equilibrium point.

One type of equilibrium, illustrated by Figure 1.4, is called a *center*, which behaves in a *neutrally stable* fashion, much like the "pathological 'frictionless-pendulum'," as May (2001) describes it. Here, a prey species and a predator species are represented by $N_1$ and $N_2$, respectively, while solid and dotted red lines represent their respective nullclines. We can observe that the equilibrium occurs at the point of intersection $(N_1, N_2) = (1,1)$ of both nullclines. (The nullclines in this case are straight lines; however, they may take the shape of any curve.) Solutions travelling on the surrounding loops represent periodic oscillations, each of which remain stable on a closed trajectory. We will survey other classifications of equilibria in the following subsection.

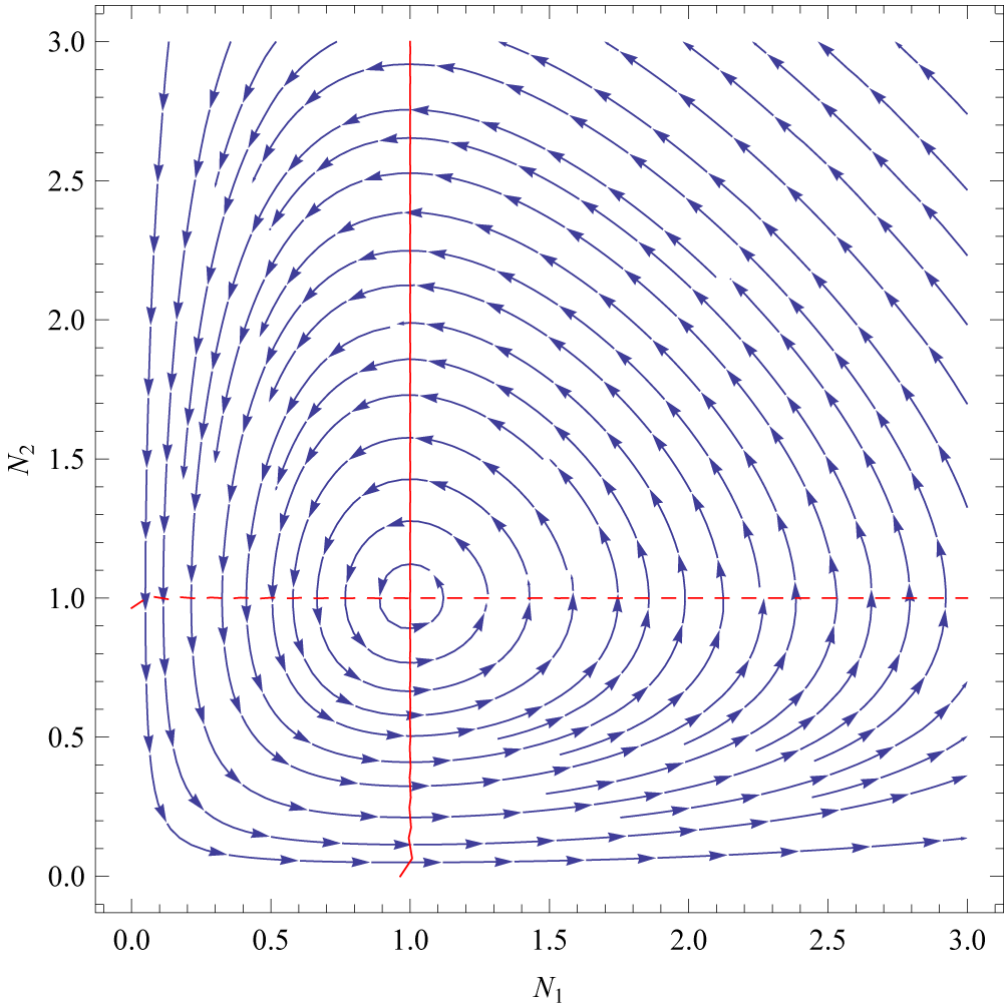


**Figure 1.4.** Phase portrait of Lotka-Volterra predator-prey system.

### *Two-Dimensional Models: Local Linearization*

The geometrical analysis considered previously indicates the existence and positioning of equilibria. A complimentary analysis involves linearizing about the system's equilibria to investigate the stability of each equilibrium point locally. In the same vein as that which we performed on one-dimensional systems, we will employ Taylor's theorem to linearize the equations in the neighborhood of the equilibrium points, and determine the characteristics of the system's equilibria (Kaplan & Glass, 1995).

Reconsider the system of equations (1.8) and (1.9):

$$\frac{dN_1}{dt} = f(N_1, N_2),$$

$$\frac{dN_2}{dt} = g(N_1, N_2).$$

Phase trajectories are solutions of

$$\frac{dN_1}{dN_2} = \frac{f(N_1, N_2)}{g(N_1, N_2)}. \tag{1.10}$$

Solutions to Eqs. (1.8) and (1.9) provide the parametric forms of the phase trajectories, where $t$ is a parameter. A unique curve passes through any arbitrary point $(\overset{0}{N}_1, \overset{0}{N}_2)$ except at equilibrium points $(N_1^*, N_2^*)$, where

$$f(N_1^*, N_2^*) = g(N_1^*, N_2^*) = 0. \tag{1.11}$$

Carrying out a Taylor series expansion of the nonlinear functions $f(N_1, N_2)$ and $g(N_1, N_2)$ in the neighborhood of the equilibrium point $(N_1^*, N_2^*)$ gives us:

$$\begin{aligned} f(N_1, N_2) &= f(N_1^*, N_2^*) + \left.\frac{\partial f}{\partial N_1}\right|_{N_1^*, N_2^*} (N_1 - N_1^*) + \left.\frac{\partial f}{\partial N_2}\right|_{N_1^*, N_2^*} (N_2 - N_2^*) + \cdots, \\ g(N_1, N_2) &= g(N_1^*, N_2^*) + \left.\frac{\partial g}{\partial N_1}\right|_{N_1^*, N_2^*} (N_1 - N_1^*) + \left.\frac{\partial g}{\partial N_2}\right|_{N_1^*, N_2^*} (N_2 - N_2^*) + \cdots, \end{aligned} \tag{1.12}$$

where ellipses represent higher-order (nonlinear) terms such as $\frac{1}{2}\frac{\partial^2 N_1}{\partial N_1^{\,2}}(N_1 - N_1^*)^2$ and $\frac{1}{2}\frac{\partial^2 N_2}{\partial N_2^{\,2}}(N_2 - N_2^*)^2$, for $f$ and $g$, respectively. If we now let

$$X = N_1 - N_1^*, \tag{1.13}$$

$$Y = N_2 - N_2^*, \tag{1.14}$$

then $\frac{dX}{dt} = \frac{dN_1}{dt}$, $\frac{dY}{dt} = \frac{dN_2}{dt}$ and $f(N_1^*, N_2^*) = 0 = g(N_1^*, N_2^*)$. The original system defined by Eqs. (1.8) and (1.9) then becomes

$$\frac{dX}{dt} = aX + bY + \cdots, \tag{1.15}$$

$$\frac{dY}{dt} = cX + dY + \cdots, \tag{1.16}$$

where $a, b, c, d$ are given by the matrix

$$\mathbf{A} = \begin{bmatrix} a & b \\ c & d \end{bmatrix} = \left[ \begin{matrix} \frac{\partial f}{\partial N_1} & \frac{\partial f}{\partial N_2} \\ \frac{\partial g}{\partial N_1} & \frac{\partial g}{\partial N_2} \end{matrix} \right]_{N_1^*, N_2^*} . \tag{1.17}$$

This is the so-called *Jacobian* matrix, which expresses via partial derivatives how each component $N_i$ of the system changes with respect to itself and all other components. In the neighborhood of the equilibrium point, the higher-order terms are negligible in comparison to the linear terms. Consequently, the nonlinear system can be approximated by a linear system.

$$\frac{dX}{dt} = aX + bY, \tag{1.18}$$

$$\frac{dY}{dt} = cX + dY. \tag{1.19}$$

The *eigenvalues* of the linearized equations describe the geometry of the vector field in the neighborhood of the equilibrium points. Let $\lambda_1$ and $\lambda_2$ be the eigenvalues of $\mathbf{A}$:

$$\det\left( \begin{bmatrix} a & b \\ c & d \end{bmatrix} - \lambda \begin{bmatrix} 1 & 0 \\ 0 & 1 \end{bmatrix} \right) = \lambda^2 - (a+d)\lambda^2 + ad - bc = 0 \quad \Rightarrow \quad \lambda_{1,2} = \frac{a+d}{2} \pm \frac{\sqrt{(a-d)^2 + 4bc}}{2}. \tag{1.20}$$

We can observe how the eigenvalues of a matrix are also related to its determinant and trace:

$$\det(\mathbf{A}) = \lambda_1 \lambda_2 \tag{1.21}$$

$$\mathrm{tr}(\mathbf{A}) = \lambda_1 + \lambda_2. \tag{1.22}$$

The eigenvalues of $\mathbf{A}$ can be found from the determinant and trace via:

$$\lambda_{1,2} = \frac{\mathrm{tr}(\mathbf{A}) \pm \sqrt{\mathrm{tr}(\mathbf{A})^2 - 4\det(\mathbf{A})}}{2}. \tag{1.23}$$

We can easily find the associated eigenvectors for each eigenvalue by solving:

$$\begin{bmatrix} a & b \\ c & d \end{bmatrix} \begin{bmatrix} N_1 \\ N_2 \end{bmatrix} = \lambda \begin{bmatrix} N_1 \\ N_2 \end{bmatrix}. \tag{1.24}$$

The eigenvalues reflect the rate of change of perturbations of size $n_i(0)$ that occur near the equilibrium point, and these rates of change occur along the eigenvectors passing through the equilibrium point. We can view the change in a perturbation as a function of the eigenvalues and eigenvectors at equilibrium:

$$n(t) = n(0)e^{\lambda_i t} = \sum_{i=1}^{k} c_i \mathbf{v}_i e^{\lambda_i t}. \tag{1.25}$$

Thus, for distinct eigenvalues, solutions are given by

$$\begin{pmatrix} N_1 \\ N_2 \end{pmatrix} = c_1 \mathbf{v}_1 e^{\lambda_1 t} + c_2 \mathbf{v}_2 e^{\lambda_2 t}, \tag{1.26}$$

where $c_1$ and $c_2$ are arbitrary constants, and $\mathbf{v}_1$ and $\mathbf{v}_2$ are the eigenvectors of $\mathbf{A}$ corresponding to their respective eigenvalues $\lambda_1$ and $\lambda_2$. If the eigenvalues are equal then $(c_1 + c_2 t)e^{\lambda t}$ describes the proportionality of the solutions. The eigenvectors are given by

$$\mathbf{v}_i = \sqrt{(1+p_i^{\,2})}\begin{pmatrix}1\\ p_i\end{pmatrix}, \qquad p_i = \frac{\lambda_i - a}{b}, \qquad b \neq 0, \qquad i = 1,2. \tag{1.27}$$

After the elimination of $t$, phase trajectories are mapped on the $(N_1, N_2)$ plane.

Several cases can be distinguished regarding the system's dynamics, depending on the state of the eigenvalues of matrix **A** in Eq. (1.17). Let us consider the resulting behaviors for various cases (see Figure 1.6).

***Classification of Equilibria***

- **Focus.** When the discriminant of Eq. (1.20) is negative, that is to say, when $\mathrm{tr}(\mathbf{A})^2 - 4\det(\mathbf{A}) < 0$, the eigenvalues are complex, or imaginary. This causes the trajectory to spiral around the equilibrium point. A focus can act as either a *sink* or *source*; i.e., its stability is classified as either stable or unstable. The imaginary part reveals how rapid the spiraling occurs, and the stability is reflected in the sign of the real part $\frac{\mathrm{tr}(\mathbf{A})}{2}$. If $\frac{\mathrm{tr}(\mathbf{A})}{2} < 0$ then the focus is stable, and if $\frac{\mathrm{tr}(\mathbf{A})}{2} > 0$ then the focus is unstable (Figure 1.6).
- **Center.** A special, limited case occurs when $\frac{\mathrm{tr}(\mathbf{A})}{2} = 0$, namely that a neutrally stable trajectory remains on a closed path circling around the equilibrium point as in (Figure 1.4). The resulting behavior is oscillations with a steady period. A perturbation of arbitrary magnitude would be required in order to move the trajectory onto a different closed path.

- **Node.** When the discriminant $\text{tr}(\mathbf{A})^2 + 4\det(\mathbf{A}) > 0$ and $\left|\text{tr}(\mathbf{A})\right| > \left|\sqrt{\text{tr}(\mathbf{A})^2 - 4\det(\mathbf{A})}\right|$, a node occurs. Here, both eigenvalues are real numbers with the same sign. If $\frac{\text{tr}(\mathbf{A})}{2} < 0$ then it is a *stable node*; if $\frac{\text{tr}(\mathbf{A})}{2} > 0$ then it is an *unstable node*.

  Additionally, we may distinguish *proper* nodes from *improper* nodes. For a stable proper node to occur, the eigenvalues must satisfy $\lambda_1 < \lambda_2 < 0$, and for an unstable proper node to occur, the eigenvalues must satisfy $\lambda_1 > \lambda_2 > 0$. A stable improper node has equal negative eigenvalues $\lambda_1 = \lambda_2 < 0,$, and an unstable improper node has equal positive eigenvalues $\lambda_1 = \lambda_2 > 0$.

- **Saddle Point.** When the discriminant $\text{tr}(\mathbf{A})^2 - 4\det(\mathbf{A}) > 0$ and $\left|\text{tr}(\mathbf{A})\right| < \left|\sqrt{\text{tr}(\mathbf{A})^2 - 4\det(\mathbf{A})}\right|$, a saddle point occurs. Here, both eigenvalues are real, but have different signs (Figure 1.6). The term "saddle point" originates from the fact that the trajectories behave in an analogous fashion as liquid poured onto a horse's saddle; there is attraction towards the point center point, followed by a perpendicular repelling away from the point as the liquid repels off the sides of the saddle (Figure 1.5).

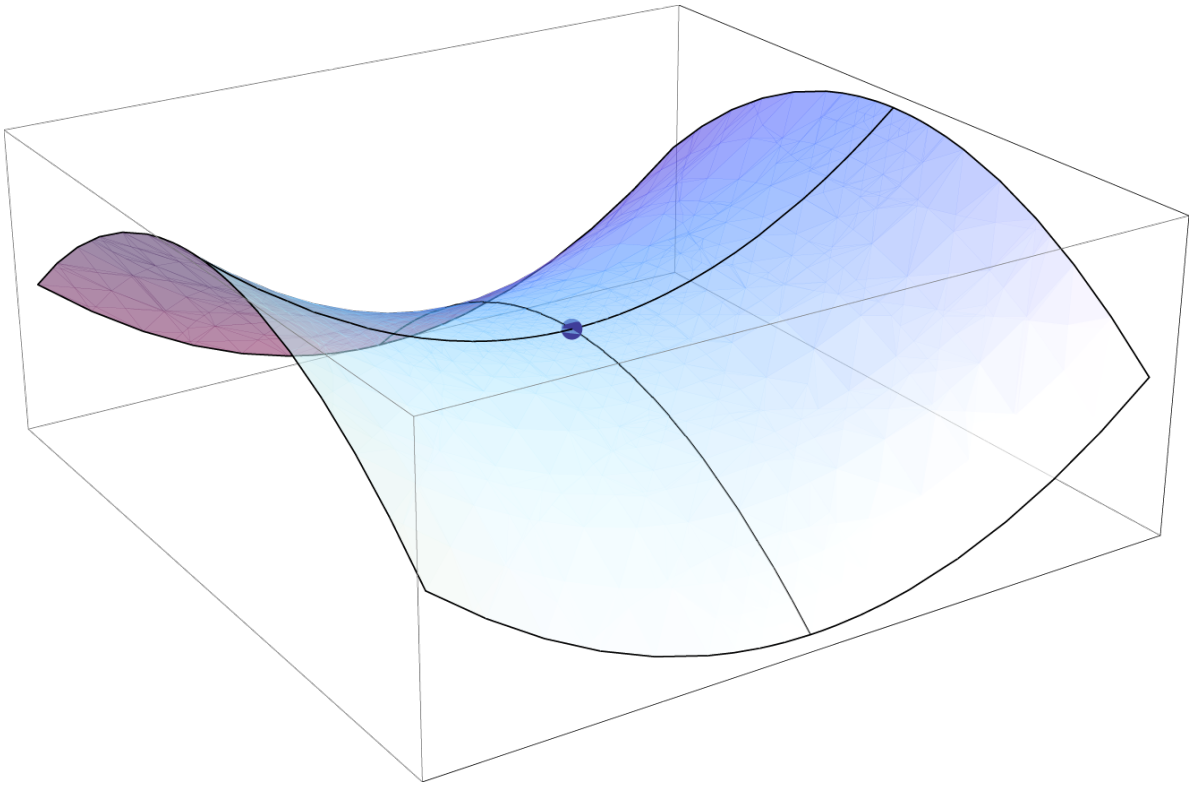

**Figure 1.5.** A saddle point (blue dot) on the graph of $z = x^2 - y^2$.

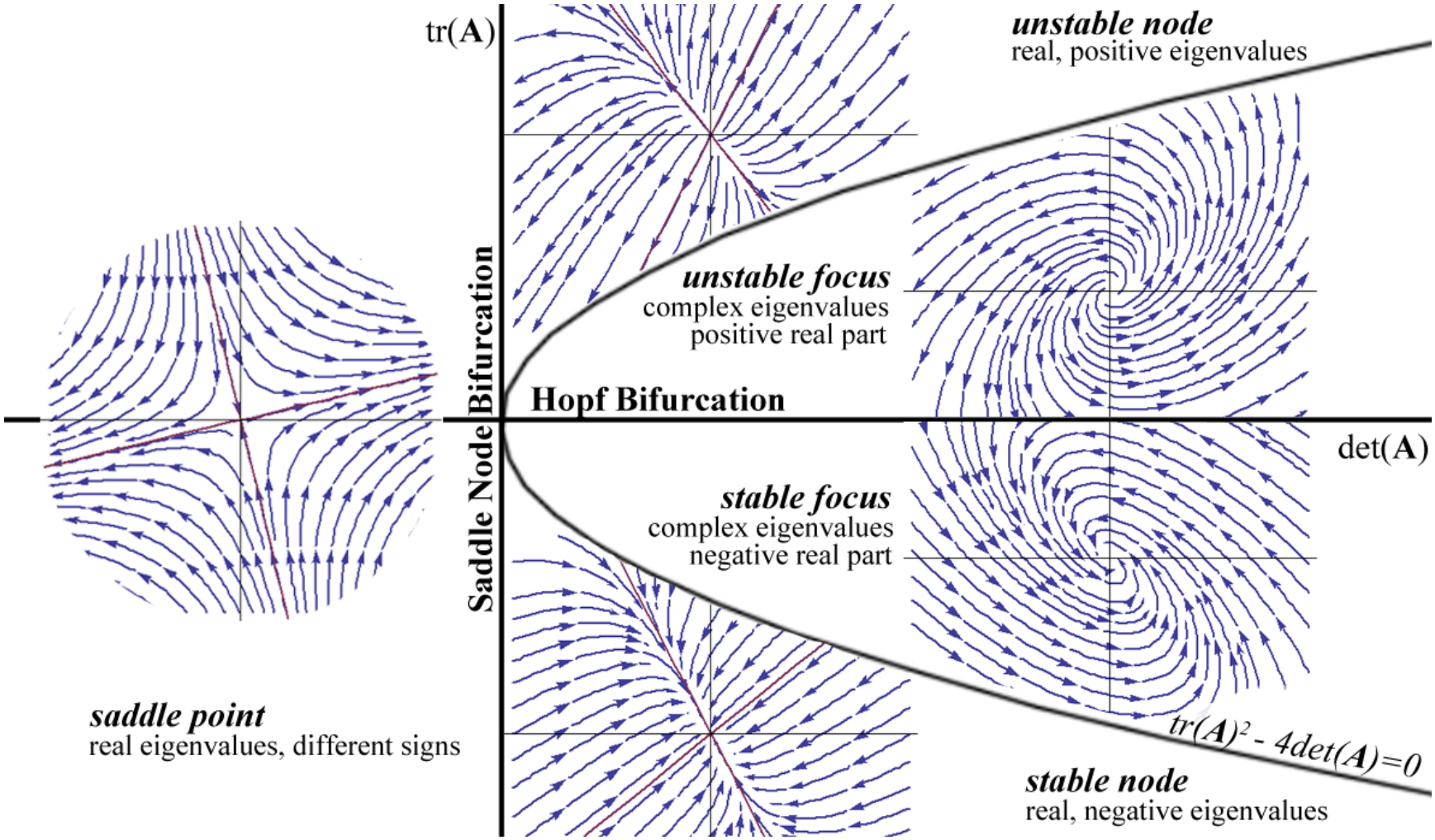


**Figure 1.6.** Classification of equilibria and their associated eigenvalues.

## 1.4 AN HISTORICAL OVERVIEW OF POPULATION DYNAMICS

The study of dynamical systems has its origins in fifteenth century physics, with Newton's invention of differential equations and solution to the two-body problem; a two-body problem is, for instance, to calculate the motion of earth around the sun given the inverse-square law of gravitational attraction between them (Strogatz, 1994). Newton and others in this time period (such as Euler, Leibniz, Gauss, and Laplace) worked to find analytic solutions to problems of planetary motion; yet, as it turned out, solutions to the three-body problem (e.g., sun, earth, and moon) were nearly impossible to achieve analytically—in contrast to the two-body problem (1994). As a result, other approaches were developed.

In the late 1800s Henri Poincaré developed many of the graphical methods still used today for analyzing the dynamics of systems that extend in complexity beyond the two-body problem. The geometrical approach pioneered by Poincaré proved to be powerful approach to finding a global, qualitative understanding of a system's dynamics (Kaplan & Glass, 1995; Strogatz, 1994).

While the geometrical approach to analyzing dynamical behaviors proved to be a powerful method, there remained an additional source of analysis that could not be well-harnessed until the rise of computing in the 1950s. With the tireless number-crunching capabilities provided by the computer, numerical methods could finally realize a far greater potential. The computer allowed one to develop a more intuitive grasp of nonlinear equations by providing rapid numerical calculations. This advancement in technology, coupled with the geometric methods of analysis, facilitated the surge of developments that

occurred in the field of nonlinear dynamics throughout the 1960s and 1970s (Strogatz, 1994).

For example, in 1963, Lorenz discovered the chaotic motion of a strange attractor. He observed that the equations of his three-dimensional system never settled down to an equilibrium state, but rather, they continued to oscillate in an aperiodic fashion (Lorenz, 1963). Additionally, running simulations from different, yet arbitrarily close, initial conditions led to unpredictably different behaviors. Plotted in 3 dimensions, the solutions to his equations fell onto a butterfly-shaped set of points (1963). It was later shown that this set contained the properties of a fractal, and his example became a major influence in chaos theory (Strogatz, 1994).

Today, the study of dynamics reaches far beyond applications in celestial mechanics, and it has achieved a truly interdisciplinary status. Significant roles have been established for studying dynamical systems in biology, chemistry, physics, cognitive science, meteorology, the social sciences, finance, philosophy, and so forth. Herein we will be considering dynamical systems solely from the standpoint of population ecology.

The following biographies are of key contributors to the study of population dynamics, with a particular emphasis on individuals whose contributions and influences are most salient in the work outlined in the following chapters, i.e., in continuous ordinary differential equation models of population dynamics. A key work used in outlining this section by Nicolas Bacaër (2011) provides a compact yet thorough account of the historical figures associated with the development of population dynamics.

***Fibonacci***

Leonardo of Pisa, who posthumously became known as Fibonacci, finished writing *Liber abaci* in 1202, in which he explained various applications of the Arabic number system (decimal) in accounting, unit conversions, interest rates, etc (Sigler, 2002). Appearing as a mere exercise in the midst of unrelated problems, Fibonacci outlined a problem that today would be described as a problem in population dynamics {Document not in library: (Bacaer, 2011a)}.

He formulated his question with regard to a pair of mating rabbits and the number of offspring that could be expected after a given period of time. He wrote the following discrete difference equation:

$$P_{n+1} = P_n + P_{n-1}, \tag{1.28}$$

which states that the number of pairs of rabbits $P_{n+1}$ after $n+1$ months is the sum of the number of pairs in month $n$ and of the number of baby pairs in month $n+1$ ; however, baby rabbits cannot reproduce; therefore, they are considered to be the pairs that were present in month $n-1$.

Fibonacci's rabbit problem was overlooked for several centuries; however, it is now recognized as one of the first models in population dynamics {Document not in library: (Bacaer, 2011a)}. While the rabbit equation (1.28) turned out to be an unrealistic model (i.e., there are no limitations on growth, no mortality, etc.), the recurrence relation that bears Fibonacci's name has an interesting relationship with naturally occurring geometries, and is found in numerous natural formations ranging from seashells to sunflowers {Document not in library: (Bacaer, 2011)}. The ratio $P_{n+1} / P_n$ approaches the so-called

golden ratio $\phi = \frac{1+\sqrt{5}}{2} \approx 1.618$ as $n \to \infty$. Despite the unrealistic nature of Fibonacci's model with regard to populations, it does share a common property with nearly all population models, namely geometrically increasing growth {Document not in library: (Bacaer, 2011)}.

***Leonhard Euler***

Leonhard Euler was a Swiss mathematician born in 1701. He made numerous contributions in the fields of mechanics and mathematics, and is considered to be one of the most prolific mathematicians of his time {Document not in library: (Bacaer, 2011a)}. Given the breadth of his work and his display of interest in demography, his work in population dynamics is only natural.

Euler stated that a population $P_n$ in year $n$ would satisfy the difference equation

$$P_{n+1} = (1+\alpha)P_n \tag{1.29}$$

where $n$ is a positive integer and the growth rate $\alpha$ is a positive real number. With an initial condition $P_0$, we find the population size in year $n$ by the equation

$$P_n = (1+\alpha)^n P_0. \tag{1.30}$$

The form of growth assumed by this equation is called geometric growth, (or exponential growth when dealing with continuous equations). As the son of a Protestant minister and having remained in strict religious faith, Euler found this growth model to suit the biblical story in Genesis which held that the entire earth's population descended from very few individuals, namely the three sons of Noah {Document not in library: (Bacaer, 2011)}. Despite this ideological alignment, however, Euler recognized that the earth would never sustain such a high rate of growth, given the fact that populations would have climbed upwards to 166 billion individuals in only 400 years. Fifty years after Euler's

formulations, Malthus considered the consequences of such growth with regard to human populations in his famous book titled *An Essay on the Principle of Population* (1798).

***Daniel Bernoulli***

Daniel Bernoulli was born in 1700 into a family of already well-established mathematicians: his father Johann Bernoulli and his uncle Jacob Bernoulli. His father did not want him to study mathematics, so Daniel began studying medicine, obtaining his doctorate in 1721 {Document not in library: (Bacaer, 2011a)}. Within four years, however, he published his first book on mathematics, titled *Exercitationes quaedam mathematicae*. After his publication, he became involved in a series of professorships in botany, physiology, and physics, and around the year 1760, Bernoulli undertook studies analyzing the benefits of smallpox inoculation given the associated risk of death from inoculation. His model held the following assumptions:

- The number of susceptible individuals $S(t)$ indicates those uninfected individuals at age $t$ who remain susceptible to the smallpox virus.
- The number of individuals $R(t)$ indicates those whom are infected with the virus but who remain alive at age $t$.
- The total number of individuals $P(t)$ equals the sum of $S(t)$ and $R(t)$.

The model's parameters $q$ and $m(t)$, respectively, represent each individual's probability of becoming infected with smallpox and each individual's probability of dying from other causes. Given these assumptions, Bernoulli derived the following ODEs:

$$\frac{dS}{dt} = -qS - m(t)S, \tag{1.31}$$

$$\frac{dR}{dt} = q(1-p)S - m(t)R. \tag{1.32}$$

The sum of these equations yields

$$\frac{dP}{dt} = -pqS - m(t)P, \tag{1.33}$$

and using Eqs. (1.31) and (1.32), he yielded the fraction of susceptible individuals at age $t$ by

$$\frac{S(t)}{P(t)} = \frac{1}{(1-p)e^{qt} + p}. \tag{1.34}$$

Bernoulli estimated the model's parameters using Edmond Halley's life table, which provided the distribution of living individuals for each age {Document not in library: (Bacaer, 2011)}. Choosing $q = 1/8$ per year, and having eliminated $m(t)$ through mathematical trickery, he computed the total number of susceptible people using Eq. (1.34) , finding that approximately 1/13 of the population's deaths was expected to be due to smallpox. He further developed his model to examine the costs and benefits of inoculation, which he concluded were undoubtedly beneficial—the life expectancy of an inoculated individual was raised by over three years. Despite these findings, the State never promoted smallpox inoculation, and ironically, the demise of King Louis XV in 1774 was a result of the smallpox virus {Document not in library: (Bacaer, 2011)}.

### *Thomas Robert Malthus*

Thomas Robert Malthus, born 1766, was a British scholar who studied mathematics at Cambridge University, obtaining his diploma in 1791, and six years later becoming a priest of the Anglican Church {Document not in library: (Bacaer, 2011a)}.

In 1798 Malthus anonymously published *An Essay on the Principle of Population, as It Affects the Future Improvement of Society, With Remarks on the Speculations of Mr. Godwin, Mr. Condorcet and Other Writers* (1798). In his book, he argued that the two named French authors' optimistic views of an ever-progressing society were flawed—particularly, they did not consider the rapid growth of human populations against the backdrop of limited resources (1798). For Malthus, the English Poor Laws, which favored population growth indirectly through subsidized feeding, did not actually help the poor, but to the contrary {Document not in library: (Bacaer, 2011a)}. Given the growth of human populations proceeding at a far greater rate than the supply of food, Malthus predicted (albeit, incorrectly) a society plagued by misery and hunger.

The so-called Malthusian growth model is described by the differential equation

$$\frac{dN}{dt} = rN, \tag{1.35}$$

where the growth of population $N$ is governed by the *net intrinsic growth rate* parameter $r \equiv b - d$, which is the rate of fertility minus the mortality rate.

Malthus emphasized that this equation holds true in capturing a growing population's dynamics only when growth goes *unchecked* (Malthus, 1798). However, the continued exponential growth of human populations against Earth's limited resources, Malthus argued, would ultimately lead to increased human suffering (1798).

Malthus' ideas proved to be influential in the work of numerous individuals, from Verhulst's density-dependent growth model to ideas of natural selection pioneered by Charles Darwin and Alfred Russel Wallace {Document not in library: (Bacaer, 2011a)}.

***Pierre-François Verhulst***

Pierre-François Verhulst was born in 1804 in Brussels, Belgium. At the age of twenty-one he obtained his doctorate in mathematics. While also bearing an interest in politics, Verhulst became a professor of mathematics in 1835 at the newly founded Free University of Brussels (Bacaër, 2011).

In 1835, Verhulst's mentor Adolphe Quetelet published *A Treatise on Man and the Development of his Faculties*; he proposed that a population's long-term growth is met with a resistance that is proportional to the square of the growth rate (Bacaër, 2011). This idea encouraged Verhulst's developments found in *Note on the law of population growth* (1838 as cited in Bacaër, 2011), in which he stated "The virtual increase of population is limited by the size and the fertility of the country. As a result the population gets closer and closer to a steady state."

Verhulst proposed the differential equation

$$\frac{dN}{dt} = rN\left(1-\frac{N}{K}\right), \tag{1.36}$$

where the growth of the population $N$ is governed by the *Malthusian parameter* $r$ and the *carrying capacity* $K$ (although at the time, these parameters were not named as such). The growth rate $r$ decreases linearly against an increasing population density $N$. However, when $N(t)$ is small compared to $K$, the equation can be approximated by the Malthusian growth equation

$$\frac{dN}{dt} \approx rN, \tag{1.37}$$

which has the solution $N(t) = N_0 e^{rt}$, where $N_0$ is the initial number of individuals in the population. However, we may also find the solution to Verhulst's "logistic" equation in Eq. (1.36) given by

$$N(t) = \frac{N_0 e^{rt}}{1 + N_0 (e^{rt} - 1)/K}, \tag{1.38}$$

which describes the growth of population $N$ increasing from an initial condition $N_0 = N(0)$ to the limit, or carrying capacity, $K$, which is reached as $t \to \infty$.

Using available demographic data for various regions, Verhulst estimated parameters $r$ and $K$ using as few as three different but equally spaced years provided through census data. He showed that if the population is $N_0$ at $t = 0$, $N_1$ at $t = T$, and $N_2$ at $t = 2T$, then both parameters can be estimated starting from Eq. (1.38), giving

$$K = N_1 \frac{N_0 N_1 + N_1 N_2 - 2N_0 N_2}{N_1^{\,2} - N_0 N_2}, \tag{1.39}$$

$$r = \frac{1}{T} \log\left[ \frac{1/N_0 - 1/K}{1/N_1 - 1/K} \right]. \tag{1.40}$$

| ANNÉES. | POPULATION. | VALEURS DE *r*. |
|---|---|---|
| 1790. . . . . | 5,930,000 | |
| 1795. . . . . | 4,618,000 | |
| 1800. . . . . | 5,306,000 | |
| 1805. . . . . | 6,275,000 | |
| 1810. . . . . | 7,240,000 | |
| 1815. . . . . | 8,439,000 | 2.147 |
| 1820. . . . . | 9,638,000 | 2.087 |
| 1825. . . . . | 11,252,000 | 2.120 |
| 1830. . . . . | 12,866,000 | 2.052 |
| 1835. . . . . | 14,964,000 | 2.076 |
| 1840. . . . . | 17,063,000 | 2.021 |

**Table 1.1** United States census data (1790 and 1840). Adapted from (Verhulst, 1845).

Verhulst's work involving the logistic equation was overlooked for several decades; however, in 1922 biologist Raymond Pearl took notice of his work after re-discovering the same equation (Pearl & Reed, 1920). In following centuries the logistic equation proved to become highly influential; for instance, it is from the logistic model's parameters *r* and *K* that r/K selection theory, pioneered by Robert MacArthur and E. O. Wilson (1967), took its name.

### *Leland Ossian Howard and William Fuller Fiske*

Leland Ossian Howard was an American entomologist who served as Chief of Bureau of Entomology for the United States Department of Agriculture (1894-1927), and W. F. Fiske headed The Gypsy Moth Project in Massachusetts (1905-1911). Howard had

been conducting research in Europe, and eventually arranged for parasites to be imported to the U.S. as agents of biological (pest) control.

As experts in the rising field of biological control, collaboration between the two individuals ensued, resulting in a new set of concepts that had been overlooked prior, namely population regulation via functional relationships. They proposed the terms "facultative" and "catastrophic" mortality, which respectively indicate different functional relationships between growth rate *r* and the population density (Howard & Fiske, 1911). Catastrophic mortality indicates a constant proportion of death in the population, regardless of density; the more familiar term for it now is *density-independence*. Facultative mortality indicates an increase of death in a population that is increasing in density, and is now more commonly referred to as *density-dependence*.

### *Raymond Pearl*

Raymond Pearl was born in Farmington, New Hampshire in 1879. After obtaining his A.B. from Dartmouth in 1899, he studied at the University of Michigan, completing his doctorate in 1902 (Jennings, 1942; Pearl, 1999). During a brief stay in Europe, Pearl studied under Karl Pearson at University College, London, where he adopted a statistical view of biological systems, and eventually, after moving to Baltimore in 1918 to become professor of biometry at the Johns Hopkins University, Pearl also became chief statistician at the Johns Hopkins Hospital (Jennings, 1942). While studying populations of *Drosophila*, he collected life expectancies, death rates, and so forth, and began discovering survivorship curves which turned out to be quite reminiscent of Verhulst's "logistic" curves (1942). While Verhulst's logistic model (Verhulst, 1845) would appear to be the precursor to

Pearl's findings, it was in fact T. Brailsford Robertson's sigmoidal-shaped chemical "autocatalytic" curve that sparked Pearl's insight (Pearl, 1999).

After showing the consistency of the survivorship curves from organisms with varying life histories, Pearl touted his finding as some *law of population growth*, which in turn sparked a considerable controversy (Kingsland, 1985).

In a paper co-published with his associate Lowell J. Reed, Pearl defended the logistic equation in its capacity to describe the growth of populations that should eventually reach a carrying capacity (Lowell & Reed, 1920):

> In a new and thinly populated country the population already existing there, being impressed with the apparently boundless opportunities, tends to reproduce freely, to urge friends to come from older countries, and by the example of their well-being, actual or potential, to induce strangers to immigrate. As the population becomes more dense and passes into a phase where the still unutilized potentialities of subsistence, measured in terms of population, are measurably smaller than those which have already been utilized, all of these forces tending to the increase of population will become reduce.

While Robertson's sigmoidal "autocatalytic" curves were too symmetrical to fit Pearl and Reed's data, they made adjustments to accommodate a more realistic fit, resulting in

$$N(t) = \frac{K}{1 + be^{at}}, \tag{1.41}$$

where population $N$ has constant parameters $b, a, K$, and, further, forming a generalized equation

$$N(t) = \frac{K}{1 + be^{\alpha t}}, \tag{1.42}$$

where $\alpha = a_1 + a_2 t^1 + \ldots + a_n t^{n-1}$. The number of terms and values of constants therefore determine the sigmoid curve's precise shape.

The logistic equation, as opposed to the curve, is most commonly written in the ODE form shown in Eq. (1.36); however, it's curve can be written

$$N(t) = \frac{K}{1 + e^{a - rt}} \tag{1.43}$$

where population $N$ is marked by the maximum rate of growth $r = r_m$, and parameters $a$ and $K$ represent the constant of integration and the carrying capacity, respectively.

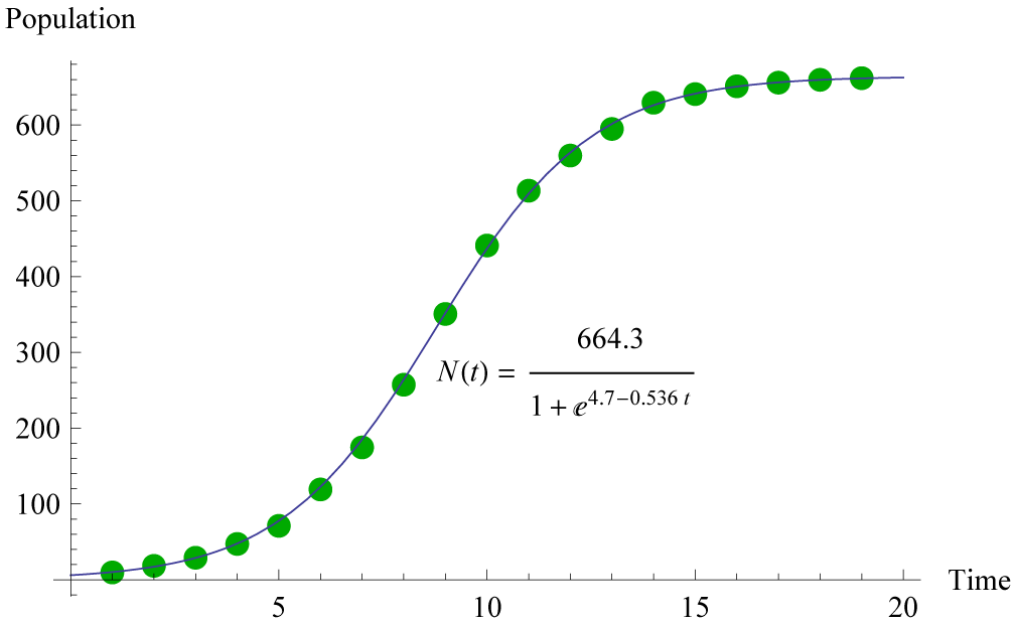


**Figure 1.7.** Logistic growth of yeast population over time. Data (green dots) collected from (Carlson, 1913 as cited in Raymond Pearl, Miner, & Parker, 1927). Logistic growth curve (blue line) fitted to data points with parameters $K = 664.3$, $a = 4.7$, and $r_m = 0.536$.

Figure 1.7 provides a visualization of the data collected from a yeast population with the corresponding fitted logistic growth curve (Carlson, 1913 as cited in Raymond Pearl, Miner, & Parker, 1927). Here, parameters were calibrated to $K = 664.3$, $a = 4.7$, and $r_m = 0.536$. Pearl also fitted logistic curves to census data of several countries including France, Sweden, and the United States (1999).

### *Alfred James Lotka and Vito Volterra*

Alfred James Lotka was born of American parents in the part of the Austro-Hungarian Empire that is now L'viv, Ukraine. He studied physics and chemistry, receiving his bachelor's from University of Birmingham in England, and eventually began work in

New York for the General Chemical Company (Bacaër, 2011). Despite his status as a physical chemist, his work has helped revolutionize the field of population ecology.

Remaining unaware of Euler's work on the subject over a century prior, Lotka began studying the dynamics of age-structured populations, first marked by the publication of "Relation between Birth Rates and Death Rates" (Lotka, 1907 as cited in Bacaër, 2011). His work follows a different approach than that of Euler, in that he uses continuous rather than discrete variables to represent age and time. Lotka's model is largely responsible for what has become known as "stable population theory" despite Euler having reached a similar result with his discrete model (Bacaër, 2011). What is meant by "stable population" is that the population's age pyramid, that is to say, the distribution of ages within the population, remains stable regardless of the population's growth or decline (2011).

Lotka's prior work involving oscillations in chemical dynamics, along with his interest in the mathematics of ecological properties, naturally led to his investigation of rhythms in ecological systems. In 1920, he published "Analytical Note on Certain Rhythmic Relations in Organic Systems," wherein he arrived at a system of equations used to describe the continuously oscillating dynamics of two populations: predators (e.g., herbivores) and prey (e.g., plants), where $X_1$ and $X_2$ represent the state of each species $S_1$ and $S_2$, respectively, for all points in time $t > 0$ (Lotka, 1920). He described the dynamics of the system verbally as:

$$\left\{\begin{matrix}\text{Rate of change of} \\ X_1 \text{ per unit of time}\end{matrix}\right\} = \left\{\begin{matrix}\text{Mass of newly formed} \\ S_1 \text{ per unit of time}\end{matrix}\right\} - \left\{\begin{matrix}\text{Mass of } S_1 \text{ destroyed} \\ \text{by } S_2 \text{ per unit of time}\end{matrix}\right\} - \left\{\begin{matrix}\text{Other dead matter} \\ \text{eliminated from } S_1 \\ \text{per unit of time}\end{matrix}\right\}$$

and

$$\left\{\begin{matrix}\text{Rate of change of} \\ X_2 \text{ per unit of time}\end{matrix}\right\} = \left\{\begin{matrix}\text{Mass of newly formed } S_2 \\ \text{per unit time (derived} \\ \text{from } S_1 \text{ as injested food)}\end{matrix}\right\} - \left\{\begin{matrix}\text{Mass of } S_2 \text{ destroyed} \\ \text{per unit of time}\end{matrix}\right\}.$$

Lotka's system of equations written in mathematical terms is thus:

$$\begin{aligned}\frac{dX_1}{dt} &= \alpha X_1 - \beta X_1 X_2 - \gamma X_1 \\ &= X_1(\Gamma - \beta X_2),\end{aligned} \tag{1.44}$$

where $\Gamma = \alpha - \gamma$, and

$$\begin{aligned}\frac{dX_2}{dt} &= \theta X_1 X_2 - \lambda X_2 \\ &= X_2(\theta X_1 - \lambda)\end{aligned} \tag{1.45}$$

where parameters $\alpha, \beta, \gamma, \theta, \lambda$ are functions of $X_1$ and $X_2$ (Lotka, 1920).

After Lotka's publication (1920) was completed, Raymond Pearl helped him obtain a scholarship from Johns Hopkins University, where Lotka was able to write his book in 1925, titled *Elements of Physical Biology* (Lotka, 1925 as cited in Bacaër, 2011). At the time, Lotka's book did not garner much attention, and it was not until Lotka's colleague Vito Volterra, who was a notable mathematical physicist, discovered the same equations that they earned their renowned status among ecologists (2011).

Vito Volterra was born in a Jewish ghetto in Ancona, Italy, although at the time the city belonged to the Papal States. While remaining poor, Volterra performed well in school, completing his doctorate in physics in 1882 and subsequently obtaining a professorship at the University of Pisa (Bacaër, 2011). Volterra received considerable attention for his work in mathematical physics, and at the age of 65 he began investigating an ecological problem proposed to him by his future son-in-law, the zoologist Umberto d'Acona. Volterra began

investigating the data collected between the years 1905 and 1923 on the varying proportions of sharks and rays landed in fishery catches in the Adriatic Sea {One or more documents not in library: (Bacaer, 2011b; Murray, 2002a)}. D'Acona had observed an increase in the populations of these predatory fishes during World War I, when harvesting activity was relatively reduced. Volterra unknowingly created the same mathematical model as Lotka's equations (1.44) and (1.45) to describe the dynamics of predator (shark) and prey (smaller fish) population. The Lotka-Volterra equations are standardly written as:

$$\frac{dN_1}{dt} = aN_1 - bN_1N_2, \tag{1.46}$$

$$\frac{dN_2}{dt} = -cN_2 + dN_1N_2, \tag{1.47}$$

where parameters $a, b, c, d > 0$. Coefficient $a$ is the growth rate of prey in the absence of predators, and $c$ is the rate of decrease of the population of predators due to starvation (i.e., in the absence of prey). The interaction terms $-bN_1N_2$ and $dN_1N_2$ express the rates of mass transfer from prey to predators, where $d \leq b$.

Lotka noticed that both populations satisfy the conditions for equilibrium in two scenarios. First, the so-called *trivial equilibrium* occurs when

$$N_1^* = N_2^* = 0, \tag{1.48}$$

where asterisks denote equilibrium. Here the prey population $N_1^*$ is extinct, and likewise, the predator population $N_2^*$, having no food source, is extinct.

Second, both populations coexist at nontrivial equilibrium when

$$N_1^* = \frac{c}{d}, \tag{1.49}$$

$$N_2^* = \frac{a}{b}. \tag{1.50}$$

However, when both populations are not at equilibrium, then both functions $N_1(t)$, $N_2(t)$ behave in an oscillatory fashion with a period $T > 0$ such that $N_1(t+T) = N_1(t)$ and $N_2(t+T) = N_2(t)$ for all $t > 0$. For instance, if there is an abundant mass of prey in population $N_1$, then the predator population $N_2$ will increase, in turn causing a decrease in $N_1$. When $N_1$ becomes too diminished to sustain feeding by $N_2$, starvation occurs, causing $N_2$ to decrease, and in turn, the mass of $N_1$ becomes rejuvenated. The process repeats itself indefinitely, resulting in temporally offset oscillations of both populations (Bacaër, 2011; Edelstein-Keshet, 2005; Kot, 2001; Murray, 2002). These equations and their counterparts are elucidated in Chapter 3.

### *Anderson Gray McKendrick and William Ogilvy Kermack*

Anderson Gray McKendrick was born in Edinburgh in 1876. He studied medicine at University of Glasgow before venturing abroad to fight diseases (namely, malaria, dysentery, and rabies) in Sierra Leone and India (Bacaër, 2011). He returned to Edinburgh in 1920 after contracting a tropical illness, and began serving as superintendent of the Royal College of Physicians Laboratory. There, McKendrick met William Ogilvy Kermack, who served as head of the chemistry division in the laboratory, and with whom McKendrick would eventually begin collaborating (2011).

In 1926, McKendrick published a paper titled “Applications of mathematics to medical problems,” in which he introduced continuous-time models of epidemics with probabilistic effects determining infection and recovery (McKendrick, 1926 as cited in

Bacaër, 2011). The paper served as the starting point for the famous S-I-R epidemic model, which was not fully developed until McKendrick and Kermack began collaborating (Kermack & McKendrick, 1927).

The S-I-R model derives its name from the progression of disease that individuals proceed through: susceptible (*S*), infected (*I*), and recovered/resistant (*R*).

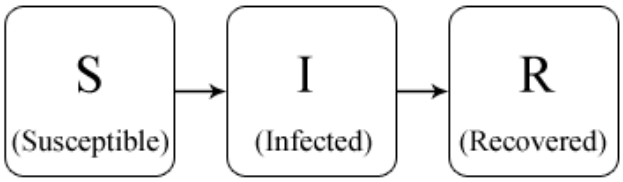


**Figure 1.8.** Kermack-McKendrick's S-I-R model. Three possible states of progression: susceptible (*S*), infected (*I*), and recovered (*R*).

A simplified form of the model demonstrating these disease dynamics follows as a three-dimensional system of equations:

$$\text{Susceptible } (S)\text{: } \frac{dS}{dt} = -\alpha SI, \tag{1.51}$$

$$\text{Infected } (I)\text{: } \frac{dI}{dt} = \alpha SI - \beta I, \tag{1.52}$$

$$\text{Recovered/resistant } (R)\text{: } \frac{dR}{dt} = \beta I, \tag{1.53}$$

where parameters $\alpha$ and $\beta$, respectively, represent the *rate of contact/infection* and the *rate of recovery* (which is proportional to the value of infected population $I$). We can see that the quantity of new individuals belonging to the infected population $I$ per unit time is proportional to the quantity of susceptible individuals and infected individuals, while those

individuals in the susceptible population $S$ are removed from $S$ as they become infected $(S \to I)$, or later on, resistant $(I \to R)$.

The total population $N(t) \equiv S(t) + I(t) + R(t)$, must begin with a set of initial conditions (since the model assumes there is no birth, death, or migration), where $S(t), I(t), R(t)$ are $\geq 0$. Thus, at the beginning of the epidemic ($t = 0$), the initial total population of size $N$ contains a proper subset of infected individuals $I(0) = I_0$, and susceptible individuals $S(0) = S_0 = N - I_0$, and we assume $R(0) = R_0 = 0$ since time must pass in order for individuals to pass from the infected state to the recovered state.

There is no analytic solution to this system; however, Kermack and McKendrick analyzed the properties of the system by other means. They observed that as $t \to \infty$, $S(t)$ decreases to a limit $S_\infty > 0$, while $I(t) \to 0$, and $R(t)$ increases to a limit $R_\infty < N$. The equation

$$-\log \frac{S_\infty}{S(0)} = \frac{\alpha}{\beta}(N - S_\infty), \tag{1.54}$$

implicitly provides $S_\infty$, and thus the final epidemic size may be obtained through $R_\infty = N - S_\infty$ (Bacaër, 2011; Kermack & McKendrick, 1927). The S-I-R model thus provides the important biological indication that an epidemic ends before all susceptible individuals become infected (2011; 1927).

Kermack and McKendrick continued developing disease models throughout the 1930s, and their work has become foundational in today's more complex epidemiological models (Bacaër, 2011; Kingsland, 1985).

***Georgy Frantsevich Gause***

Georgy Frantsevich Gause was a Russian biologist born in Moscow in 1910. He began his undergraduate studies at Moscow University under advisor W. W. Alpatov who was a student and friend of Raymond Pearl. Professor Alpatov may be credited for the direction of Gause's work, specifically in experimental population ecology (Kingsland, 1985).

Foregoing field studies in favor of the controlled laboratory environment, Gause was able to control for potentially confounding variables in a series of ecological experiments performed *in vitro*. In one experiment, two competing species of *Paramecium* displayed typical logistic growth when grown in isolation; however, when placed together *in vitro*, one species always drove the other to extinction (Gause, 1934). By shifting environmental resource parameters (e.g., food and water), Gause found that the "winner" and "loser" species were not somehow predestined but rather dependent on the values of the resource parameters. Similar results were yielded in experiments between two competing species of *Saccharomyces* yeast (Gause, 1932).

These findings led to what has been called the *principle of competitive exclusion*, or *Gause's principle*; stated briefly: "complete competitors cannot coexist" (Hardin, 1960). Restated, if two sympatric non-breeding populations (i.e., separate species occupying the same space) occupy the *same* ecological niche, and Species 1 has even an infinitesimally slightest advantage over Species 2, then Species 1 will eventually overtake Species 2, leading towards either extinction or towards an evolutionary shift to a different ecological niche for the less-adapted species. As Hardin's "First Law of Ecology" states, "You cannot do only one thing."

Additionally, Gause's results were a confirmation of Lotka-Volterra's competition model, which, by design, upholds the exclusion principle by assuming normal logistic growth for each species grown in isolation, and for species placed together, the mutually-inhibitory effect of each species' population (given the appropriate competition parameters) leads to the eventual demise of the "disadvantaged" population (Robert MacArthur & Levins, 1967). The phenomenon is also called "limiting similarity" (1967). The Lotka-Volterra competition model is described by the coupled system of equations:

$$\frac{dN_1}{dt} = r_1 N_1 \left[ 1 - \frac{\left( N_1 + \alpha_{12} N_2 \right)}{K_1} \right], \tag{1.55}$$

$$\frac{dN_2}{dt} = r_2 N_2 \left[ 1 - \frac{\left( N_2 + \alpha_{21} N_1 \right)}{K_2} \right], \tag{1.56}$$

where populations of Species 1 and Species 2 are represented by $N_1$ and $N_2$, respectively. This model and its counterparts are considered in further detail in Section 3.1.

# CHAPTER 2: SINGLE-SPECIES POPULATION MODELS

The dynamics of single populations are generally described in terms of one-dimensional differential equations. In this chapter, we consider one-dimensional population models that were developed over the past several centuries to describe the growth and/or decay of single homogeneous populations. There is a pedagogical aim here in asserting the simple and fundamental principles at work in most continuous population models, and in this vein, we will begin from very simple foundations.

Following a progression similar to that taken in Edelstein-Keshet's text *Mathematical Models in Biology* (2005), we aim to elucidate the development of various models by augmenting in gradual increments. The addition of each new parameter will be accompanied by an empirical and/or theoretical justification that will, in any case, provide the reader with a gradual (as opposed to what one might call *saltationist*) sense of the model's evolution.

It should be noted that, in most scenarios, the models outlined herein are inaccurate and oversimplified. They do not consider stochasticity (chance events), environmental effects, spatial heterogeneity, or age-structure. With regard to stochasticity, it is assumed that the deterministic model will produce results that, on average, would be produced by the analogous stochastic model (Maynard Smith, 1974).

The absence of certain realistic features does not negate the importance of these models or the principles they convey. Whereas the illustrative power of the models

outlined below is pedagogical in nature; therefore, the explanatory power of the underlying principles, in large part, dominates the striving we might otherwise have for realism or accuracy.

## 2.1 MALTHUSIAN EXPONENTIAL GROWTH MODEL

Recalling from Section 1.4, Thomas Robert Malthus proposed that a population's growth will proceed exponentially if growth goes unchecked (1798). The Malthus equation is denoted

$$\frac{dN}{dt} = rN, \tag{2.1}$$

where $N$ represents the number of individuals in the population (or more precisely, the *biomass* of the population) and $r$ is a constant representing the intrinsic rate of growth. The growth rate $r$ is also called the *Malthusian parameter* or the *net intrinsic growth rate* (i.e., $r \equiv b - d$, where *b* and *d* are intrinsic birth and death rates, respectively).

Units of time $t$ vary depending on the organism of inquiry. For instance, for rapidly multiplying organisms (e.g., bacteria), *t* may be measured in minutes, whereas for slowly multiplying organisms (e.g., elephants), *t* may be measured in years.

### *Analytic Solution*

The solution to Eq. (2.1) is easily achieved by separation of variables and integrating both sides of the equation, assuming that $N(0) = N(t = 0)$, to yield

$$\int_{N(0)}^{N(T)} \frac{dN}{N} = \int_{t=0}^{t=T} r dt \tag{2.2}$$

$$\ln \left| N \right\|_{N(0)}^{N(T)} = rt + c \Big|_0^T, \tag{2.3}$$

and evaluating the upper and lower limits yields

$$\begin{aligned} \ln N(T) - \ln N(0) &= (rT + c) - (r * 0 + c), \\ \ln\big(N(T)\big) - \ln\big(N(0)\big) &= rT \\ \frac{N(T)}{N(0)} &= e^{rT}, \end{aligned} \tag{2.4}$$

where $N(T)$ and $N(0)$ are both positive. Rearranging the equation, we get the exact solution

$$N(t) = N_0 e^{rt}, \tag{2.5}$$

where the *initial condition* $N(0) = N_0$.

***Geometrical Analysis***

Malthusian growth described by Eq. (2.1) can manifest as both exponential growth and exponential decay (Figure 2.1); for instance, exponential growth occurs for all $r > 0$ (Figure 2.2); however, reversing the sign of *r*, the model becomes one in which a population decays exponentially in time as the fraction *r* of individuals is removed per unit time (Figure 2.3).

Viewing the phase line (Figure 2.1), the linear rate of change in population size, or density, is portrayed for both exponential growth and exponential decay. The only equilibrium solution $\frac{dN}{dt} = 0$ occurs when $N^* = 0$. Qualitatively, we can judge the equilibrium point's stability based on whether trajectories approach $+\infty$, for all $r > 0$ or zero for all $r < 0$.

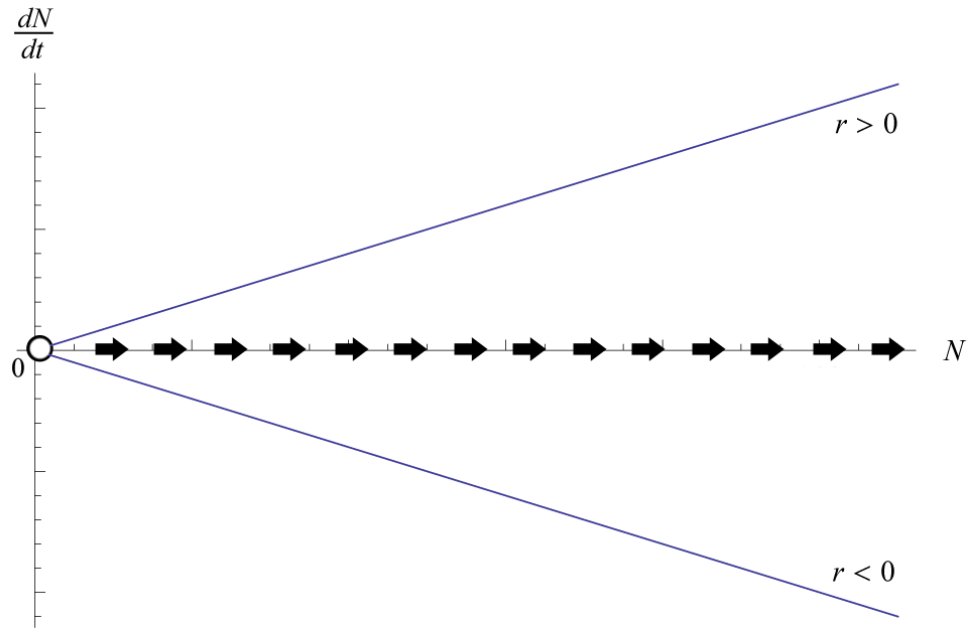


**Figure 2.1.** Phase line portrait of exponential model given by Eq. (2.1): phase trajectory reveals the linear rate of change in growth as a function of $N$.

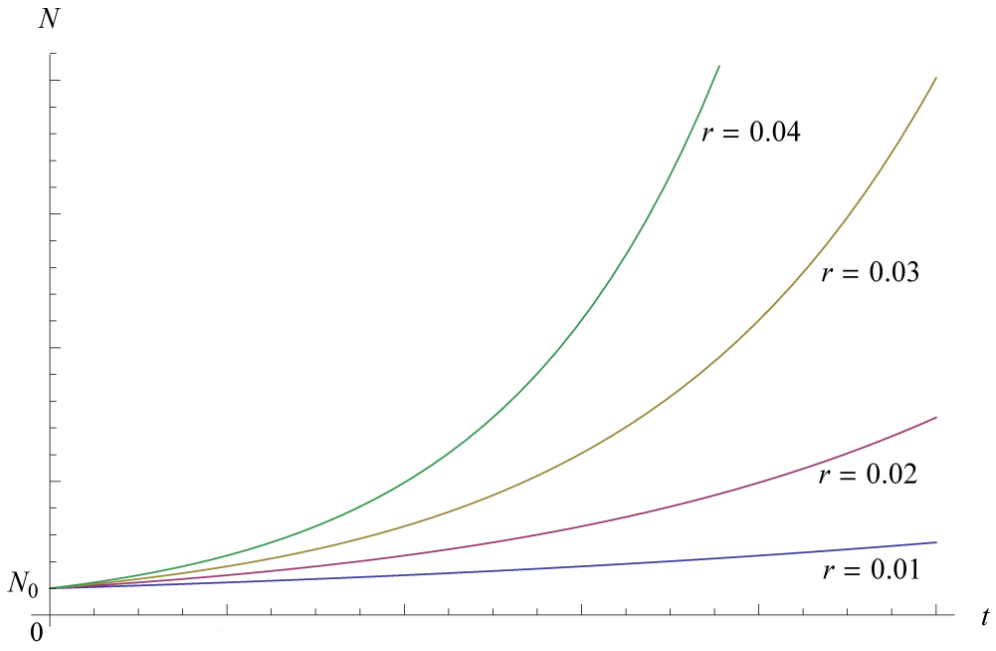


**Figure 2.2.** Dynamics of exponential growth given by Eq. (2.1): exponential growth for a set of arbitrary positive growth rates $r$.

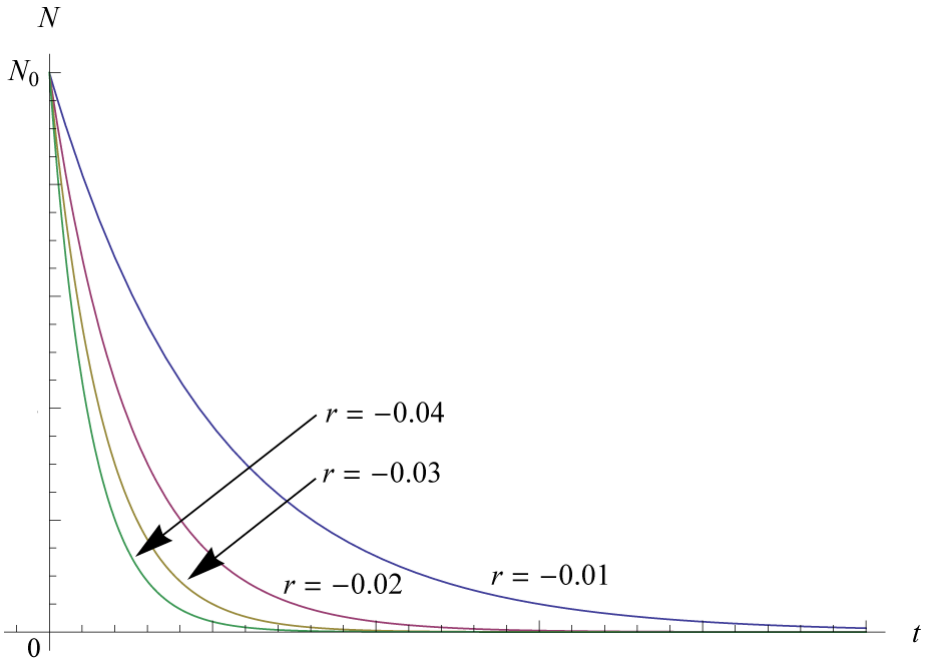


**Figure 2.3.** Dynamics of exponential growth described by Eq. (2.1): exponential decay for a set of arbitrary negative growth rates $r$.

### *Assumptions of the Model*

The Malthus model is one of the simplest models of growth for any reproducing population; however, it is too simple to be useful in most circumstances. As such, it makes the following assumptions: the population is homogeneous (i.e., all members are identical); the population inhabits a uniform and unvarying environment; an infinite supply of nutrients is available; there are no spatial limitations, and growth is density-independent. Realistically, population growth is limited by various factors from resource availability to predation. Additional limitations arise from the system's internal dynamics, such as overcrowding. The Malthus model may accurately describe the growth of a population for a limited period of time; however, unrestrained growth is never sustainable, and thus additional components are necessary to obtain a more realistic model.

## 2.2 CLASSICAL LOGISTIC GROWTH MODEL

The logistic equation, developed by Verhulst (Section 1.4), anticipates a limit, or *carrying capacity*, on population growth. This carrying capacity is symbolically represented $K$. Plotting the population's growth as a function of time shows $N$ approaching $K$ along a sigmoid (*S*-shaped) curve when the population's initial state $N_0$ is below $\frac{K}{2}$; above $\frac{K}{2}$, solutions exponentially converge towards $K$ (Figure 2.5). The addition of the new term $K$ to our model is an intuitive advance from the Malthusian model since we know realistically that individuals cannot propagate infinitely in a finite space, and that the growth rate should decline as population density increases.

The classic logistic model assumes that the individual growth rate ($r_a$) is a linearly decreasing function of $N$ such that

$$r_a = f(N). \tag{2.6}$$

We define $r_m$ as the maximum growth rate, which should decrease linearly as *N* increases. When $N = K$, the rate of growth will be zero, and growth rate will become negative in the case of $N > K$. This new linearly decreasing growth rate is developed starting with an equation for a straight line $y = ax + b$, where *a* represents the slope and *b* is the y-intercept (here $r_m$).

We calculate the slope by

$$a = \frac{y_2 - y_1}{x_2 - x_1} = \frac{0 - r_m}{K - 0} = -\frac{r_m}{K}, \tag{2.7}$$

and the relationship between $r_a$ and *N* is

$$r_a = r_m\left(1-\frac{N}{K}\right). \tag{2.8}$$

Now we may substitute $r_a$ for $r$ in the original equation given in Eq. (2.1) to yield the logistic equation:

$$\frac{dN}{dt} = r_m N\left(1-\frac{N}{K}\right). \tag{2.9}$$

***Analytic Solution***

The solution to Eq. (2.9) may be achieved via separation of variables and integrating both sides, assuming $N(t=0) = N(0)$, to yield

$$\frac{dN}{N\left(1-\frac{N}{K}\right)} = rdt, \tag{2.10}$$

$$\int_{N(0)}^{N(T)} \frac{dN}{N\left(1-\frac{N}{K}\right)} = \int_{t=0}^{t=T} rdt. \tag{2.11}$$

Integrating requires the use of partial fractions:

$$\begin{aligned} \frac{1}{N(1-\frac{N}{K})} &= \frac{A}{N} + \frac{B}{(1-\frac{N}{K})}, \\ 1 &= A\left(1-\frac{N}{K}\right) + BN, \\ 1 &= A - \frac{AN}{K} + BN, \end{aligned} \tag{2.12}$$

where $A=1$ and $\frac{-A}{K+B} = 0$, and further, we get

$$\begin{aligned} B &= \frac{A}{K} = \frac{1}{K}, \\ \int_{N(0)}^{N(T)} \frac{dN}{N} + \int_{N(0)}^{N(T)} \frac{dN}{K(1-\frac{N}{K})} &= \int_0^T rdt. \end{aligned} \tag{2.13}$$

Integration and exponentiation on both sides yields

$$\begin{aligned} \ln N(T) - \ln N(0) - \ln\left(1 - \frac{N(T)}{K}\right) + \ln\left(1 - \frac{N(0)}{K}\right) &= rT, \\ \exp\left[\ln N(T) - \ln N(0) - \ln\left(1 - \tfrac{N(T)}{K}\right) + \ln\left(1 - \tfrac{N(0)}{K}\right)\right] &= e^{rTT}, \end{aligned} \tag{2.14}$$

and further simplifying, we get

$$\begin{aligned} \frac{\exp\left[\ln N(T)\right]\exp\left[\ln\left(1 - \tfrac{N(0)}{K}\right)\right]}{\exp\left[\ln N(0)\right]\exp\left[\ln\left(1 - \tfrac{N(T)}{K}\right)\right]} &= e^{rt}, \\ \frac{N(T)(1 - \tfrac{N(0)}{K})}{N(0)(1 - \tfrac{N(T)}{K})} &= e^{rt}. \end{aligned} \tag{2.15}$$

Finally, solving for $N(T)$ and simplifying further provides us with the solution:

$$N(T) = \frac{N_0 K}{N_0 + (K - N_0)e^{-rt}}, \tag{2.16}$$

where the initial condition $N(0) = N_0$.

### *Obtaining Equilibrium Points*

We obtain the system's equilibrium points $N^*$ by finding all values of $N$ that satisfy $\frac{dN}{dt} = 0$:

$$\begin{aligned} \frac{dN}{dt} = 0 \qquad &\Rightarrow \qquad r_m N^* \left(1 - \frac{N^*}{K}\right) = 0, \\ r_m N^* = 0 \qquad &\text{or} \qquad \left(1 - \frac{N^*}{K}\right) = 0, \end{aligned} \tag{2.17}$$

and we get

$$N^* = 0, \tag{2.18}$$

$$N^* = K. \tag{2.19}$$

Thus, the logistic equation has exactly two equilibrium points.

| $N$ | $dN/dt$ |
|---|---|
| $N > K$ | $\frac{dN}{dt} < 0$ |
| $0 < N < K$ | $\frac{dN}{dt} > 0$ |
| $N = K$ | $\frac{dN}{dt} = 0$ |
| $N = 0$ | $\frac{dN}{dt} = 0$ |

**Table 2.1.** Behavior logistic growth, described by Eq. (2.9), for different cases of $N$.

***Geometrical Analysis***

Viewing the phase line in Figure 2.1 we can discern a number of facts concerning the system's dynamics; in fact, we see that the equilibria are already obtained graphically. We can also observe that any point $N_0$ on the trajectory will approach $K$ as $t \to \infty$, with the exception of the case $N = 0$, in which there is no population. Table 2.1 illustrates the sign of $\frac{dN}{dt}$ for values of $N$.

The trivial equilibrium point $N^* = 0$ is unstable, and the second equilibrium point $N^* = K$ represents the stable equilibrium, where $N$ asymptotically approaches the carrying capacity $K$. In terms of the limit, we can say $\lim_{T \to \infty} N(T) = K,\ N(0) > 0$.

A point of inflection occurs at $N = \frac{K}{2}$ for all solutions that cross it, and we can see graphically that growth of $N$ is rapid until it passes the inflection point $N = \frac{K}{2}$. From there, subsequent growth slows as $N$ asymptotically approaches $K$.

As shown in Table 2.1, if $N > K$, then $\frac{dN}{dt} < 0$, and $N$ decreases exponentially towards $K$. This case should only occur when the initial condition $N(0) = N_0 > K$. In the

following section we will confirm the stability of equilibria by linearization about each equilibrium solution.

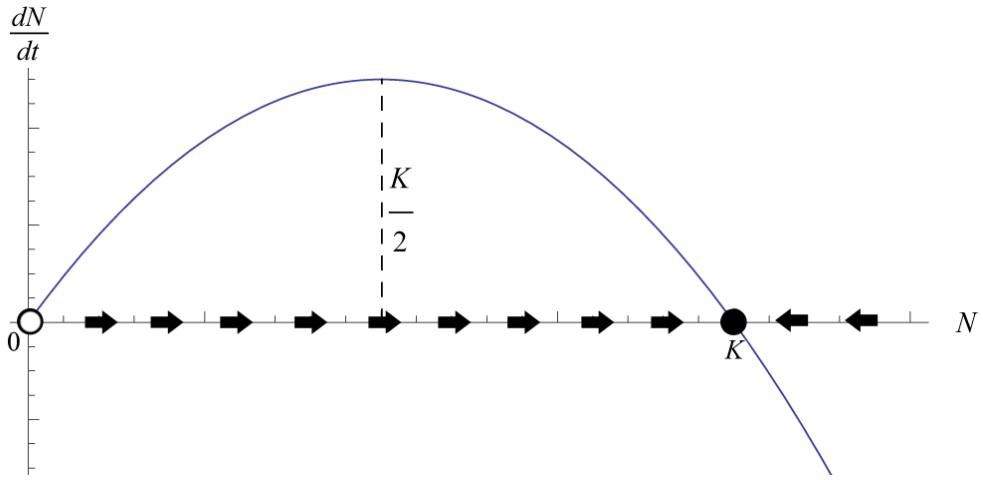


**Figure 2.4.** Phase line portrait of logistic growth, as described by Eq. (2.9).

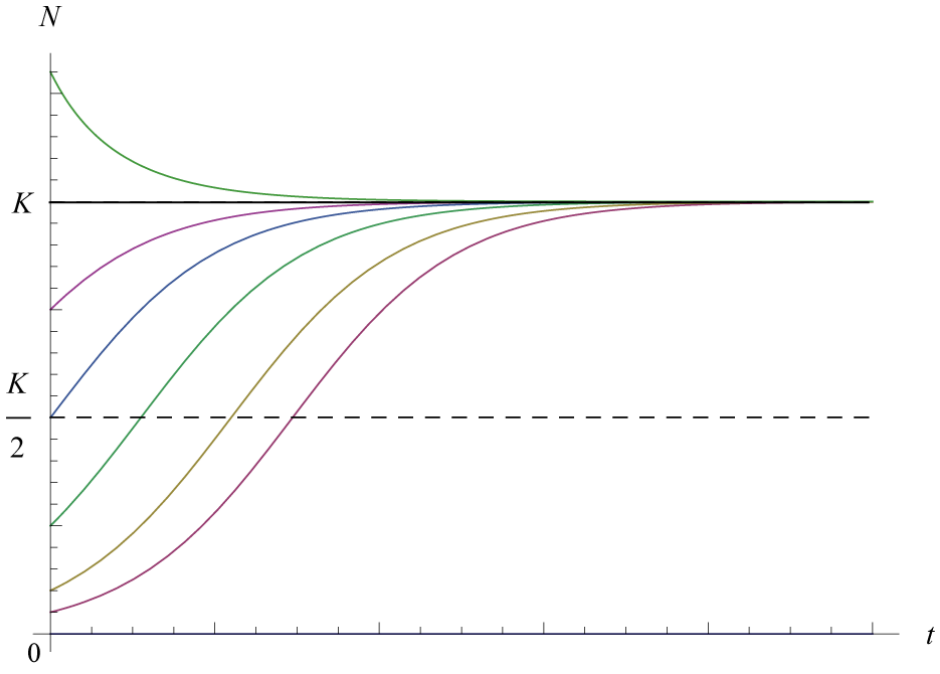


**Figure 2.5.** Dynamics of the logistic model given by Eq. (2.9).

***Local Linearization***

For a more quantitative measure of the system's stability, we may linearize the equation in the neighborhood of its equilibrium points. Let $n(t) = N(t) - N^*$ where $n(t)$ is a small perturbation in the neighborhood of an equilibrium point denoted $N^*$. We are interested in whether the perturbation grows or decays, so consider

$$\frac{dn}{dt} = \frac{d}{dt}(N - N^*) = \frac{dN}{dt} = f(N) = f(N^* + n). \tag{2.20}$$

Performing a Taylor series expansion on Eq. (2.20) yields

$$f(N^* + n) = f(N^*) + n\left.\frac{df}{dN}\right|_{N=N^*} + \cdots, \tag{2.21}$$

where ellipsis denotes quadratically small nonlinear terms in $n$ that we will henceforth ignore. We may also eliminate the term $f(N^*)$ since it is equal to zero, and we are provided with the approximated equation

$$f(N^* + n) \approx n\left.\frac{df}{dN}\right|_{N=N^*}. \tag{2.22}$$

Thus,

$$f(N) = r_m N\left(1 - \frac{N}{K}\right) = r_m N - \frac{r_m N^2}{K}, \tag{2.23}$$

$$\frac{df(N)}{dN} = r_m - \frac{2r_m N}{K}. \tag{2.24}$$

Hence, near the equilibrium points $N^* = 0$ and $N^* = K$, we obtain

$$\frac{dn}{dt} \approx n\left(r_m - \frac{2r_m N}{K}\right)\Bigg|_{N=0} = r_m n, \tag{2.25}$$

$$\frac{dn}{dt} \approx n\left( r_m - \frac{2r_m N}{K} \right)\Bigg|_{N=K} = n(r_m - 2r_m) = -r_m n. \tag{2.26}$$

Recalling the Malthus equation from previously, we see that $\frac{dn}{dt} \approx \pm r_m n$ takes its form. Since $r_m > 0$, these results indicate that the equilibrium point $N^* = 0$ is unstable since the perturbation $n(t)$ grows exponentially if $f'(N^*) > 0$. On the other hand, $N^* = K$ is stable since $n(t)$ decays exponentially if $f'(N^*) < 0$.

Additionally, the magnitude of $f'(N^*)$ tells how rapidly exponential growth or decay will occur, and its reciprocal $\left| f'(N^*) \right|^{-1}$ is called the *characteristic time scale*, which gives the amount of time it takes for $N(t)$ to vary significantly in the neighborhood of $N^*$ (Strogatz, 1994). In this case, the characteristic time scale is $\left| f'(N^*) \right|^{-1} = r_m^{-1}$ for both equilibrium points.

***Assumptions of the Model***

The assumptions of the logistic model are the same as those of the Malthusian model, except that the reproduction rate is positively proportional to the size of the population when the population size is small and negatively proportional when the population is large. The point $K$ towards which the population converges is the carrying capacity, and the parameter $K$ is determined phenomenologically.

As Sewall Wright cautioned, "any flexible mathematical formula resulting in a sigmoid shape could be made to fit the data" (Kingsland, 1985). Thus it would not be difficult to produce a curve fitted to the data by producing an algebraic expression and simply deriving a differential equation from which it is the solution (Murray, 2002).

## 2.3 THETA LOGISTIC GROWTH MODEL

A simple variation on the classic logistic model incorporates a new term $\theta$, which provides additional generality and flexibility in terms of the change in per-capita growth rate $r_a$ with respect to population density $N$. With this augmentation, the model may yield more fitting results under circumstances where density-dependence is of importance. As such, the model provides additional complexity over the classic logistic model in terms of the shape of its growth curve (Figures 2.6 and 2.7).

The updated per-capita growth rate parameter becomes

$$r_a = r_m\left[1-\left(\frac{N}{K}\right)^{\theta}\right], \tag{2.27}$$

where $\theta > 0$. Note that zero-growth would be given by $\theta = 0$, and in cases where $\theta < 0$, growth under $K$ would decay to 0, while growth above $K$ would proceed unbounded. The respective convexity or concavity of the curve is determined by whether $\theta > 1$ or $\theta < 1$ (Figure 2.6).

Substituting the updated per-capita growth rate $r_a$ into the original logistic equation yields the theta-logistic growth model:

$$\frac{dN}{dt} = r_m N\left[1-\left(\frac{N}{K}\right)^{\theta}\right]. \tag{2.28}$$

Varying the parameter $\theta$ is intended to reflect relation between intraspecific competition and population density. As such, the linear density dependence held by the classical logistic model can be altered to become curvilinear (Figure 2.6). This is clear because

$$\begin{aligned}(r_a N)^{\theta} &> r_a N, \quad \theta > 1 \\ (r_a N)^{\theta} &= r_a N, \quad \theta = 1 \\ (r_a N)^{\theta} &< r_a N, \quad \theta < 1.\end{aligned} \tag{2.29}$$

That is to say, if we set $\theta > 1$, the carrying capacity term will be given more weight, in turn, weakening the density-dependence for low values of $N$, and thus reflecting scenarios in which crowding holds a lesser prominence (since crowding has a lesser effect at low densities). When $\theta = 1$, the model is identical to the classic logistic model, so its density dependence is a linearly decreasing function of $N$. When $\theta < 1$, density-dependence is strengthened for low values of $N$, leading to slowed population growth (Figures 2.6 and 2.7). Mechanistically, the value of $\theta$ should depend on the functional relationships between individuals at varying densities; however the parameter is phenomenological, and therefore, does not possess a mechanistic significance *per se*.

Analyzing time-series data from ~3200 different populations of insects, birds, mammals, and fish using the Global Population Dynamics Database, Sibly, et al. (2005) found respective theta values for each population using a least-squares approach. In the majority of cases (~75%), populations displayed a concave-up density-functional relationship (i.e., $\theta < 1$), indicating that many animals spend the majority of their time at or above carrying capacity (2005).

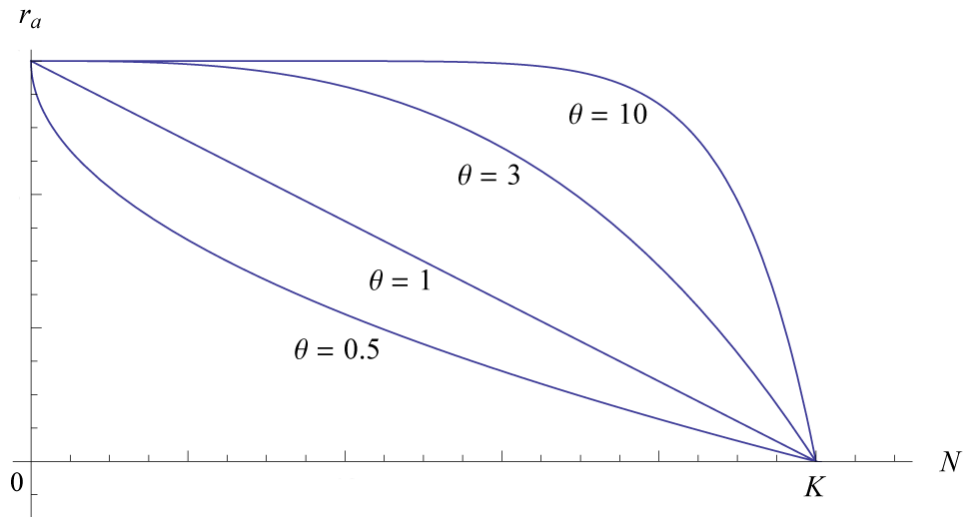


**Figure 2.6.** Plot of per-capita growth rate $r_a$, described by Eq. (2.27), as a function of population density $N$ for arbitrary values of $\theta = (0.5,\ 1,\ 3,\ 10)$.

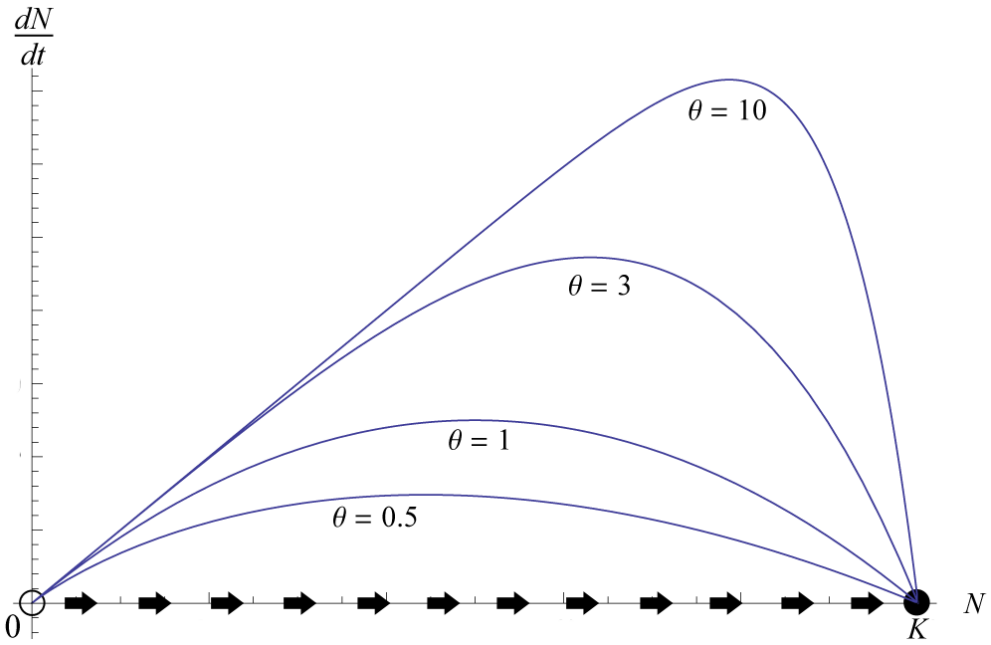


**Figure 2.7.** Phase line portrait of theta-logistic model, described by Eq. (2.28), for arbitrary values of $\theta = (0.5,\ 1,\ 3,\ 10)$.

## 2.4 LOGISTIC MODEL WITH ALLEE EFFECT

We now consider an elaborated derivation of the logistic model intended to describe the situations in which a sparsity of individuals leads in turn to the reduced survival of offspring. Restated in biological terms, the *Allee effect* is said to occur when dwindling population levels lead, in turn, to increasingly diminished reproduction, despite the lack of intraspecific competition (Figure 2.8). In fisheries science literature, the effect is often called *depensation* (Courchamp, Clutton-Brock, & Grenfell, 1999).

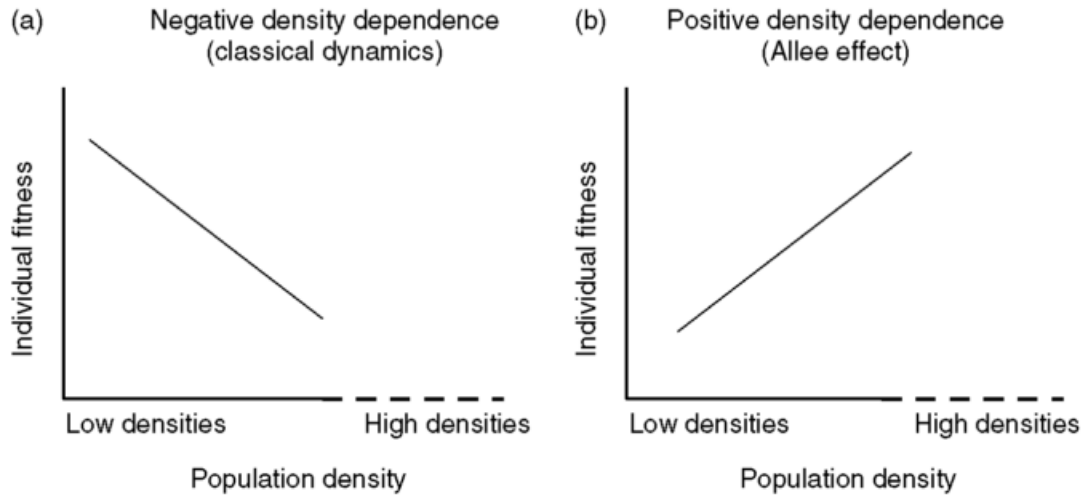


**Figure 2.8.** Schematic plot of (a) negative (classical "logistic-type") and (b) positive (Allee effect) relationships between individual fitness and population density. *Note*. Adapted from (Courchamp, Luděk, & Gascoigne, 2008).

Allee effects can be explained by several mechanisms, including limited mate availability and impaired cooperative behavior (for instance, if too few individuals are available for cooperative foraging, hunting, and defense). Courchamp, Luděk, & Gascoigne (2008) devote a whole chapter in *Allee Effects in Ecology and Conservation* to elucidating such mechanisms.

The Allee effect is evidenced to occur in numerous species ranging from the colonial Damaraland mole-rats to African Wild Dogs (Courchamp, Clutton-Brock, & Grenfell, 1999), although it is not believed to affect the populations of most taxa (Sibly, Barker, Denham, Hone, & Pagel, 2005). A good review of the Allee effect is provided by Courchamp, *et al.* (1999).

To begin incorporating the Allee effect into our model, we set out to find a *critical threshold value* (also called the *Allee threshold*), above which the population will continue by ordinary logistic growth, and below which the population will decay.

Consider a population following normal logistic growth. We begin by reversing the sign of the right-hand-side of Eq. (2.9) to yield

$$\frac{dN}{dt} = -r_m N\left(1-\frac{N}{K}\right), \tag{2.30}$$

where $r_m > 0$. As before, there are still two fixed-points, only their stabilities have reversed; now $N^* = 0$ is stable and $N^* = K$ is unstable. Finally, incorporating the Allee threshold parameter $T$ yields

$$\frac{dN}{dt} = -r_m N\left(1-\frac{N}{T}\right)\left(1-\frac{N}{K}\right), \tag{2.31}$$

where $r_m > 0$ and $0 < T < K$ (Gruntfest, *et al.*, 1997 as cited by Courchamp, Luděk, & Gascoigne, 2008).

As expressed previously, the stability of equilibrium points can be assessed qualitatively by analyzing the phase line portrait and additionally by linearizing the equation in the neighborhood of its equilibrium points.

***Geometrical Analysis***

The phase line portrait (Figure 2.9) depicts all three equilibrium solutions of Eq. (2.31). (We will rely solely on this graphical method of determination while keeping in mind that equilibria can be found just as easily algebraically.) Stable equilibria are found at $N^* = 0$ and $N^* = K$, and a single unstable equilibrium lies at $N^* = T$. Solutions starting above the unstable equilibrium $N^* = T$ converge to $K$ as $t \to \infty$, and those below $N^* = T$ converge to zero as $t \to \infty$.

The concavity or convexity of the solution curves (Figure 2.10) is determined in the usual manner by finding the slope of the line tangent to the curve of the phase line (Figure 2.9). Points of inflection occur where the slope of the line tangent to the phase line equals zero. Here, the first point of inflection is found between zero and $T$, and the other is found between $T$ and $K$. Relative degrees of local stability may be distinguished by determining the steepness of the slopes around each equilibrium point, respectively.

We observe that the behavior of Eq. (2.31) reflects that of an Allee effect insofar as individuals below the Allee threshold $T$ become extinct and those above the threshold progress towards their environmental carrying capacity $K$. The specific type is called a *strong* Allee effect because populations below the threshold are driven to extinction, whereas, in cases of a *weak* Allee effect, populations below the threshold are merely hampered in their rates of growth.

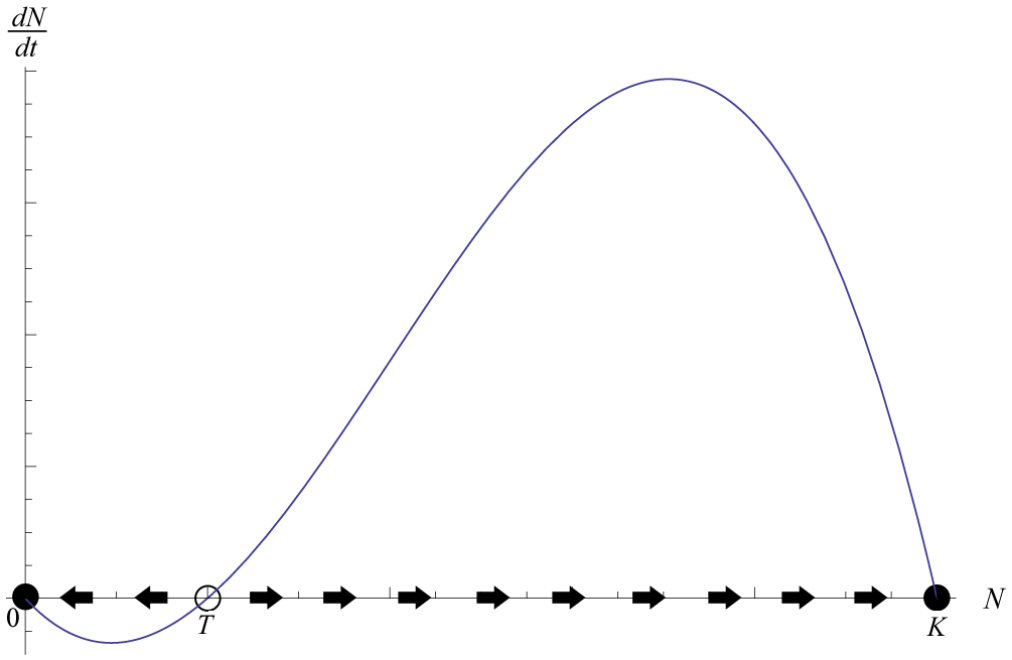


**Figure 2.9.** Phase line portrait of the Allee effect, as described by Eq. (2.31), where $T$ represents the critical Allee threshold value and $K$ represents carrying capacity.

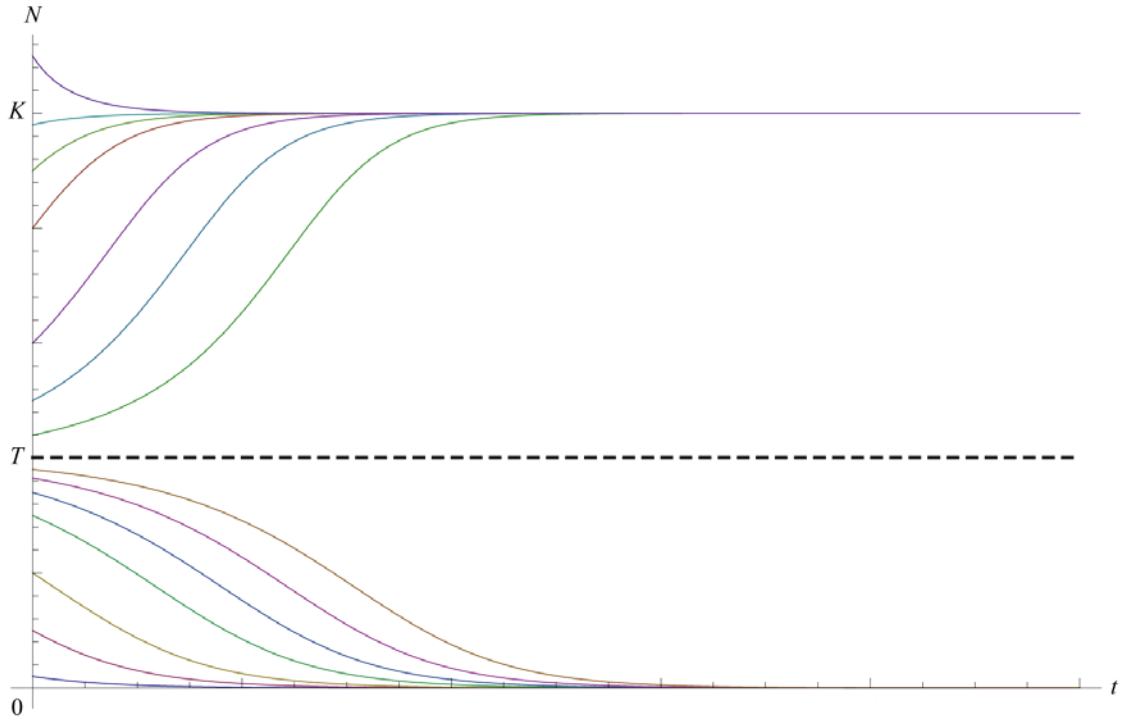


**Figure 2.10.** Dynamics of the Allee effect, as described by Eq. (2.31), where $T$ represents the critical Allee threshold value and $K$ represents carrying capacity.

## 2.5 GROWTH MODEL WITH MULTIPLE EQUILIBRIA

In the models outlined thus far, populations always return to the same state of equilibrium following a perturbation (unless they are pushed to extinction). *Multistability* is the possibility of alternative nontrivial equilibria such that the timing and magnitude of a disturbance may push the population into an alternate equilibrium state.

Recalling the heuristic rolling-ball analogy from Section 1.1, we can imagine a landscape upon which the ball is placed, where dips in the landscape represent basins of attraction, towards which the ball will roll, and mounds in the landscape represent unstable domains that repel the ball. In the current model, there are two basins of attraction towards which the ball might roll, depending on its positioning in the landscape; i.e., there are two stable nontrivial equilibria. If the population is at equilibrium, then a perturbation of sufficient magnitude is required in order for the population to converge towards the alternate equilibrium.

Eq. (2.31) of the prior model possesses two nontrivial equilibria; however, the threshold equilibrium $T$ is unstable, so there remains only one stable nonzero equilibrium solution. Augmenting Eq. (2.31) such that a new term $\left(1-\frac{N}{L}\right)$ is included, and reversing the sign of the right-hand side of the equation, we obtain

$$\frac{dN}{dt} = r_m N\left(1-\frac{N}{T}\right)\left(1-\frac{N}{K}\right)\left(1-\frac{N}{L}\right), \tag{2.32}$$

where $0 < T < K < L$ and $r_m > 0$.

In general, we may consider an equation of the form

$$\frac{dN}{dt} = r_m N \prod_{i=1}^{n} \left( 1 - \frac{N}{K_i} \right), \tag{2.33}$$

having $n$-many equilibrium points, where $K_1 < K_2 < \ldots < K_n$. Equilibrium points occur at $N^* = K_i$, with alternating stability such that $N^* = K_{2i}$ are stable and $N^* = K_{2i+1}$ are unstable.

***Geometrical Analysis***

Figures 2.11 and 2.12 reveal the existence of two unstable equilibria ( $N^* = 0$ and $N^* = K$ ) and two stable equilibria ( $N^* = T$ and $N^* = L$ ) of Eq. (2.32). The population may persist at either of the two alternative stable equilibria. If the population contains any number of individuals initially, then it is guaranteed to converge towards *one* of the equilibria, such that if the population's size $N$ is below the ecological threshold $K$, then it will converge towards the "lower" equilibrium $T$, and if $N > K$, then it will converge towards the "higher" equilibrium $L$.

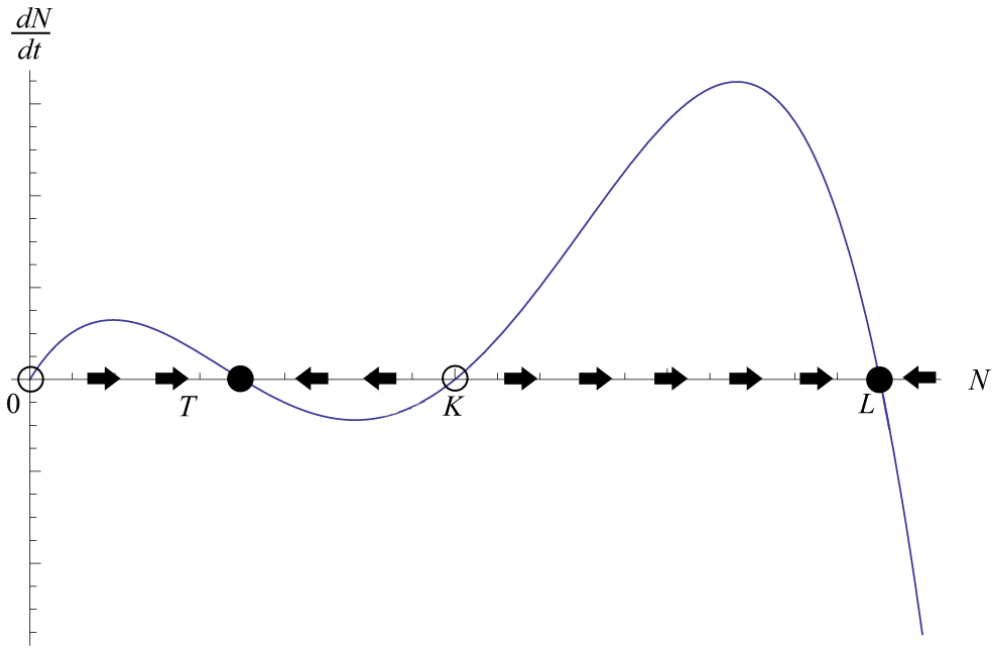


**Figure 2.11.** Phase line portrait of multistable growth model, given by Eq. (2.32), with potential for coexistence at two levels, $T$ and $L$, where $T < L$.

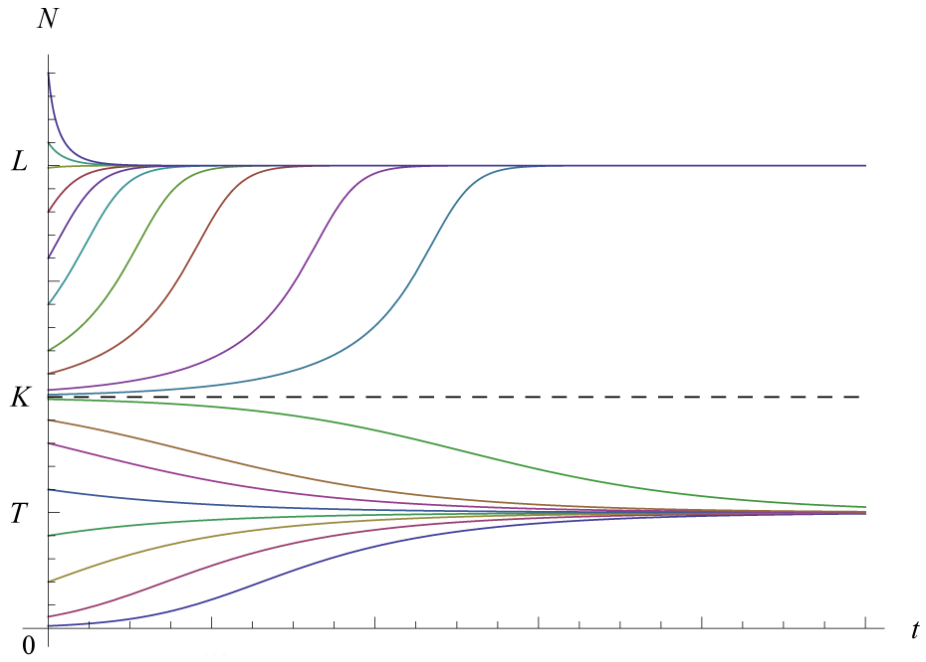


**Figure 2.12.** Dynamics of multistable growth model, given by Eq. (2.32), with potential for coexistence at two levels, $T$ and $L$ where $T < L$.

# CHAPTER 3: MULTISPECIES POPULATION MODELS

Until this point, our models have assumed that the population of a single species is constitutive of the entire system. We previously considered one-dimensional models wherein single homogeneous populations fluctuate in the absence of interspecific relationships. Naturally, ecosystems are constituted by populations belonging to *multiple* species, and thus, the effects of these species on one another should come under consideration.

The narrowest case in which community dynamics can be modeled involves two interacting species. These two species are modeled under the assumption that everything apart from that pair (that is to say, the environment, other species, etc.) is held constant. Therefore, the two species are said to exist in *isolation*. Maynard Smith (1974) presents an important inquiry, "Does the extent to which actual ecosystems show properties of persistence or stability depend on the fact that the pairwise interactions between species would likewise, in isolation, lead to stability and persistence?"

Henceforth we turn our considerations to two-dimensional models, which will allow us to account for the effects of two species on one another. We will explore the ecological ramifications of competing populations, mutualistic populations, and predator-prey interactions, all of which exhibit characteristic nonlinear behaviors. Using qualitative approaches outlined prior, we will aim to elucidate these models and their ecological

significance. Additionally, we will make use of the Jacobian (community) matrix of partial derivatives and its eigenvalues to assess the systems and their stability.

Ecological relationships are typically categorized by virtue of their interspecific interactions. Table 3.1 describes these categories, most important of which are competition, mutualism, commensalism, and predation. The term *symbiosis* describes the interactions of species acting within the limits of any of these criteria; however, the term is restrictive insofar as species must live together in order to be called *symbiotic*.

| Interaction type | Effect on Species 1 | Effect on Species 2 |
|---|---|---|
| **Competition** | (–) Negative | (–) Negative |
| **Mutualism** | (+) Positive | (+) Positive |
| **Predation** | (+) Positive | (–) Negative |
| **Commensalism** | (+) Positive | (0) Neutral |
| **Amensalism** | (–) Negative | (0) Neutral |
| **Indifference** | (0) Neutral | (0) Neutral |

**Table 3.1.** Basic categories of interspecific relationships.

The (+) positive, or *accelerating*, effect on a species $S$ should be read as an increase in the birth rate of $S$, or otherwise a decrease in the death rate of $S$. Along the same lines, the (–) negative, or *inhibitory*, effect on a species $S$ should be read as a decrease in the birth rate of $S$ or an increase in the death rate of $S$.

The interaction types in Table 3.1 may be placed into three broad categories: cooperation, competition, and predation. We may broadly categorize competitive behaviors as those which occur when multiple species compete for the same commodity or resource. This may take the form of competitive exclusion (– –) or more rarely, amensalism (– 0). By contrast, cooperative behaviors are those having a positive net effect on the species

involved, namely mutualism (+ +) and commensalism (+ 0). Examples of two forms of mutualism are provided in Sections 3.2 and 3.3.

Lastly, it should be noted that according to these classifications, *predation* subsumes both predator-prey interactions and host-parasitoid interactions. This assumption is favorable in terms of its simplicity, but it has the unfortunate consequence of emphasizing predation over analogous interactions such as parasitism or herbivore-plant interactions (Maynard Smith, 1974). We will distinguish these terms on a case-by-case basis.

## 3.1 INTERSPECIFIC COMPETITION MODEL

A major ecological concern involves competition between species sharing a habitat. How does a population's rate of change depend on its own population density and on the densities of competitor populations? We will begin with a classical model of competition based on the work of Lotka and Volterra wherein two species are assumed to have an inhibitory effect on each other.

We start with the assumption that two species with respective populations $N_1$ and $N_2$ each grow logistically in the absence of the other, as described by the following uncoupled logistic equations:

$$\frac{dN_1}{dt} = r_1 N_1 \left(1 - \frac{N_1}{K_1}\right), \tag{3.1}$$

$$\frac{dN_2}{dt} = r_2 N_2 \left(1 - \frac{N_2}{K_2}\right). \tag{3.2}$$

The terms $N_i / K_i$ for $i = 1, 2$ can be understood to represent *intra*specific competition, as we recall from the logistic model. The carrying capacity parameter $K$, therefore, is not explicitly determined by the environment, and thus its connection with the environment (including other species) is determined phenomenologically (Pastor, 2008).

If $N_1$ and $N_2$ are two species competing for a shared resource, however, then we may assume that the carrying capacity becomes a shared resource. As a result, each species inhibits the other: each individual of the first species causes a decrease in per capita growth of the second species, and *vice versa*. The result is a *symmetrical* system of equations; that is, symmetrical with respect to the identity of each species (Pastor, 2008). This symmetry is

sensitive to parameters $K_1, K_2$, as well as the pair of competition coefficients $\alpha, \beta$, which describes the degree of competition each species has on the other. We arrive at the following coupled system of equations:

$$\frac{dN_1}{dt} = r_1 N_1 \left[ 1 - \frac{\left( N_1 + \alpha N_2 \right)}{K_1} \right], \tag{3.3}$$

$$\frac{dN_2}{dt} = r_2 N_2 \left[ 1 - \frac{\left( N_2 + \beta N_1 \right)}{K_2} \right], \tag{3.4}$$

where $r_1, r_2, K_1, K_2, \alpha$, and $\beta$ are positive.

### *Obtaining Equilibrium Points*

Next, we may obtain the system's equilibrium points by finding values of $N_1$ and $N_2$ for which $\frac{dN_1}{dt} = \frac{dN_2}{dt} = 0$ is satisfied. We may begin by finding values for which $\frac{dN_1}{dt} = 0$:

$$\begin{aligned} &\frac{dN_1}{dt} = 0 \quad \Leftrightarrow \quad r_1 N_1^* \left( 1 - \frac{N_1^* + \alpha N_2^*}{K_1} \right) = 0, \\ &N_1^* = 0 \quad \text{or} \quad N_1^* = K_1 - \alpha N_2^*. \end{aligned} \tag{3.5}$$

Finding values for which $\frac{dN_2}{dt} = 0$ is satisfied:

$$\frac{dN_2}{dt} = 0 \quad \Leftrightarrow \quad r_2 N_2^* \left( 1 - \frac{N_2^* + \beta N_1^*}{K_2} \right) = 0, \tag{3.6}$$

and, plugging in the first value $N_1^* = 0$ in Eq. (3.5), into Eq. (3.6), it is apparent that

$$N_2^* = 0 \quad \text{or} \quad N_2^* = K_2. \tag{3.7}$$

Plugging the second value from Eq. (3.5), $N_1^* = K_1 - \alpha N_2^*$, into Eq. (3.6), we get

$$r_2 N_2^* \left( 1 - \frac{N_2^* + \beta K_1^* - \alpha\beta N_2^*}{K_2} \right) = 0 \tag{3.8}$$

and values of $N_2^*$ satisfying Eq. (3.8) are

$$N_2^* = 0 \quad \text{and} \quad N_2^* = \frac{K_2 - \beta K_1}{1 - \alpha\beta}.$$

We can identify the following equilibrium points:

$$\left(N_1^*, N_2^*\right) = (0, 0) \tag{3.9}$$

$$\left(N_1^*, N_2^*\right) = (K_1, 0) \tag{3.10}$$

$$\left(N_1^*, N_2^*\right) = (0, K_2) \tag{3.11}$$

$$\left(N_1^*, N_2^*\right) = \left(\frac{K_1 - \alpha K_2}{1 - \alpha\beta}, \frac{K_2 - \beta K_1}{1 - \alpha\beta}\right) \tag{3.12}$$

We should note that the equilibrium in Eq. (3.12) may not be positive for all possible values; however, a biologically relevant equilibrium must be positive. With this information at hand, we may continue our analysis by determining the stability of each equilibrium point, and viewing the qualitative behaviors for each case.

### *Geometrical Analysis*

The *nullclines*, or *zero-growth isoclines*, of these equations allow us to better characterize the system's dynamics. Nullclines for $N_1$ and $N_2$ occur, respectively, where

$$\frac{dN_1}{dt} = 0 \text{ and } \frac{dN_2}{dt} = 0. \tag{3.13}$$

The $N_1$ nullclines $\left(\frac{dN_1}{dt} = 0\right)$ are given by the equations

$$N_1 = 0, \tag{3.14}$$

$$N_1 = K_1 - \alpha N_2, \tag{3.15}$$

and the $N_2$ nullclines $\left(\frac{dN_2}{dt} = 0\right)$ are given by

$$N_2 = 0, \tag{3.16}$$

$$N_2 = K_2 - \beta N_1. \tag{3.17}$$

We may already see how nullclines could become helpful in finding equilibrium solutions. In Figures 3.5-3.6, nullclines are represented as dashed and solid red lines for $N_1$ and $N_2$, respectively. The general behavior of the vector field depends on whether the nullclines intersect, their degrees of orientation, and their relative positioning. In addition, we may assess the stability of each equilibrium point to determine the flow of trajectories in the phase plane.

From the phase portraits illustrated in Figures 3.2-3.6, we can observe the outcomes delineated in Table 3.2, and the parameter space diagram of Figure 3.1.

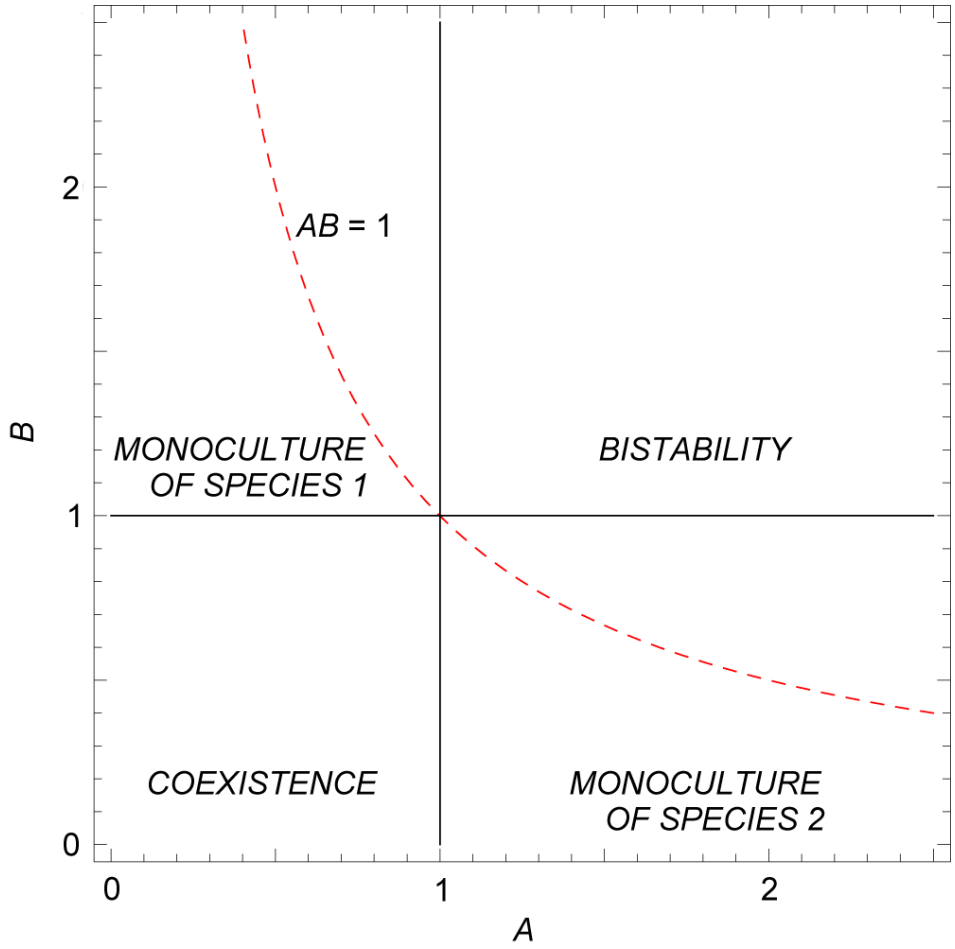


**Figure 3.1.** Parameter space of four competition scenarios, where, $A = \alpha \frac{K_2}{K_1}$ and $B = \beta \frac{K_1}{K_2}$.

| Value of $\alpha, \beta$ | Qualitative Observation | Corresponding Figure |
|---|---|---|
| $\alpha < \frac{K_1}{K_2}, \beta > \frac{K_2}{K_1}$ | *Competitive advantage*: $N_1$ prevails, $N_2$ goes extinct. | 3.2, 3.3 |
| $\alpha > \frac{K_1}{K_2}, \beta < \frac{K_2}{K_1}$ | *Competitive advantage*: $N_2$ prevails, $N_1$ goes extinct. | 3.4 |
| $\alpha > \frac{K_1}{K_2}, \beta > \frac{K_2}{K_1}$ | *Strong competition*: Bistability: winner's success depends on initial conditions. | 3.5 |
| $\alpha < \frac{K_1}{K_2}, \beta < \frac{K_2}{K_1}$ | *Weak competition*: Coexistence: both populations remain in stable equilibrium. | 3.6 |

**Table 3.2.** Four possible scenarios of the Lotka-Volterra competition model.

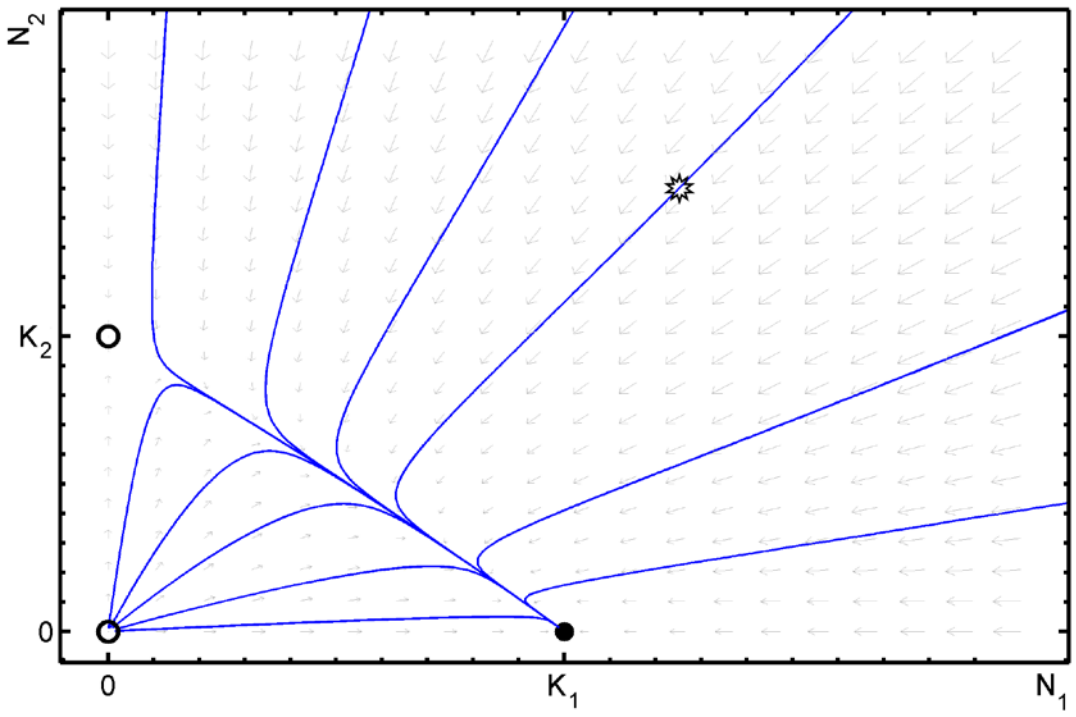


**Figure 3.2.** Phase plane portrait of Lotka-Volterra competition model, described by Eqs. (3.1) and (3.2), for $\alpha < \frac{K_1}{K_2}, \beta > \frac{K_2}{K_1}$, indicating a competitive advantage of $N_1$ over $N_2$.

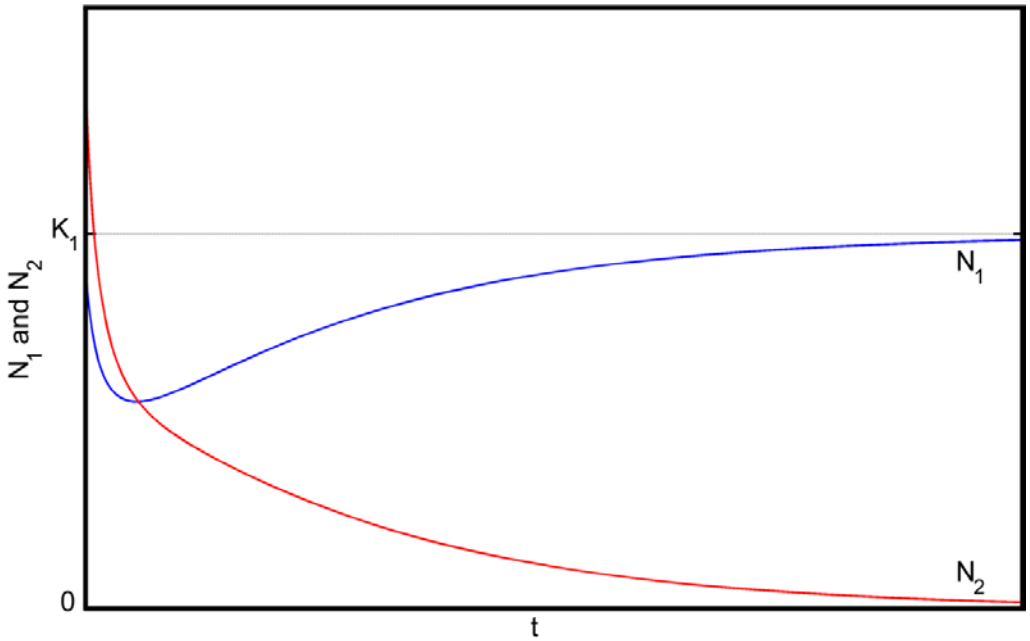


**Figure 3.3.** Dynamics of Lotka-Volterra competition model, described by Eqs. (3.1) and (3.2), for $\alpha < \frac{K_1}{K_2}, \beta > \frac{K_2}{K_1}$. The corresponding solution curve is denoted by ✸ in Figure 3.2. Here, $N_1 \to N_1^* \neq 0$ and $N_2 \to N_2^* = 0$ as $t \to \infty$.

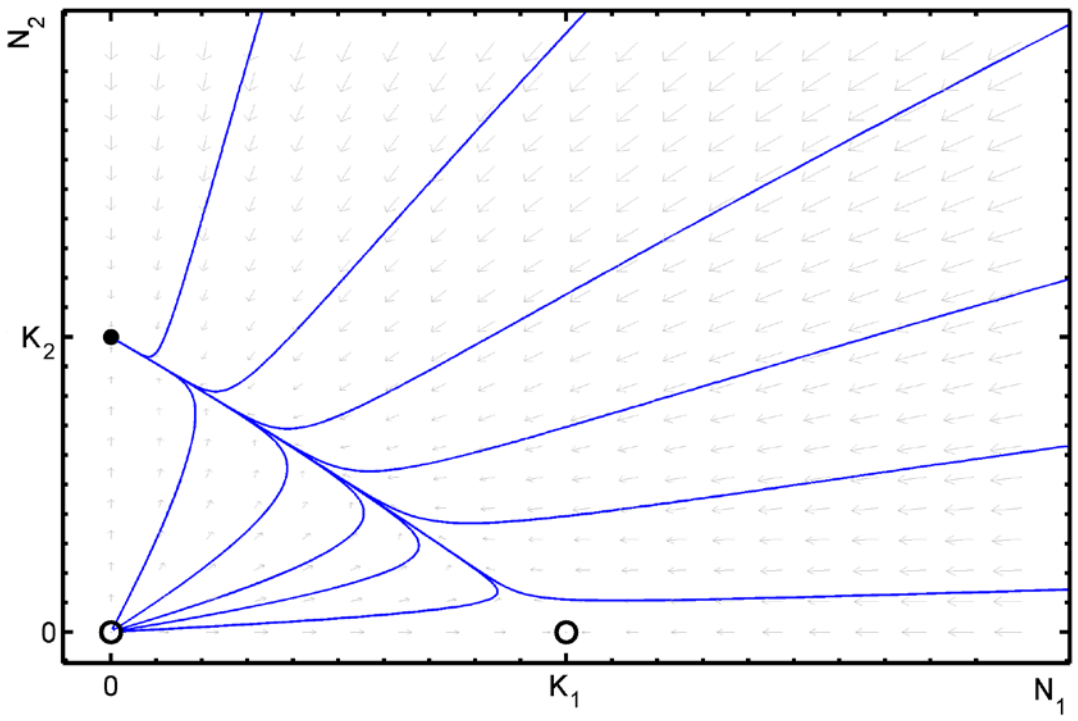


**Figure 3.4.** Phase plane portrait of Lotka-Volterra competition model, described by Eqs. (3.1) and (3.2), for $\alpha > \frac{K_1}{K_2}, \beta < \frac{K_2}{K_1}$, indicating a competitive advantage of $N_2$ over $N_1$.

In the phase plane portraits of the two monoculture scenarios (Figures 3.2 and 3.4), there are no critical points in the first quadrant because the nullclines for $N_1$ and $N_2$ (not shown) do not intersect. The equilibria for both cases lie on the axes/boundaries, so they are called *boundary equilibria* (Pastor, 2008). The solid dots represent nodal sinks (stable), and the hollow dots represent nodal sources (unstable).

Under the conditions $\alpha < \frac{K_1}{K_2}, \beta > \frac{K_2}{K_1}$, which we may rewrite as $K_1 > \alpha K_2$ and $K_2 < \beta K_1$, we observe that the maximum carrying capacity of $N_1$, namely $K_1$, exceeds that of $N_2$ when the maximum competitive effect of $N_2$ is less than the maximum carrying capacity of $N_1$; thus, the $N_1$ nullcline is positioned above that of $N_2$ in the phase plane, and the trajectories converge toward stable equilibrium at $(N_1^*, N_2^*) = (K_1, 0)$ (Figure 3.2).

The reverse case is also true; under the conditions $\alpha > \frac{K_1}{K_2}, \beta < \frac{K_2}{K_1}$, the $N_2$ nullcline is positioned above that of $N_1$, and trajectories converge towards a stable boundary equilibrium at $(N_1^*, N_2^*) = (0, K_2)$ (Figure 3.4). These results uphold Gause's *principle of competitive exclusion*; namely that when the competitive effect of species $N_1$ does not overcome the carrying capacity $K_2$ of species $N_2$, then $N_1$ will be driven toward extinction, resulting in a monoculture of $N_2$, or *vice versa*. This type of competition is referred to as *interference* competition (Hardin, 1960; Meszéna, *et al.* 2006).

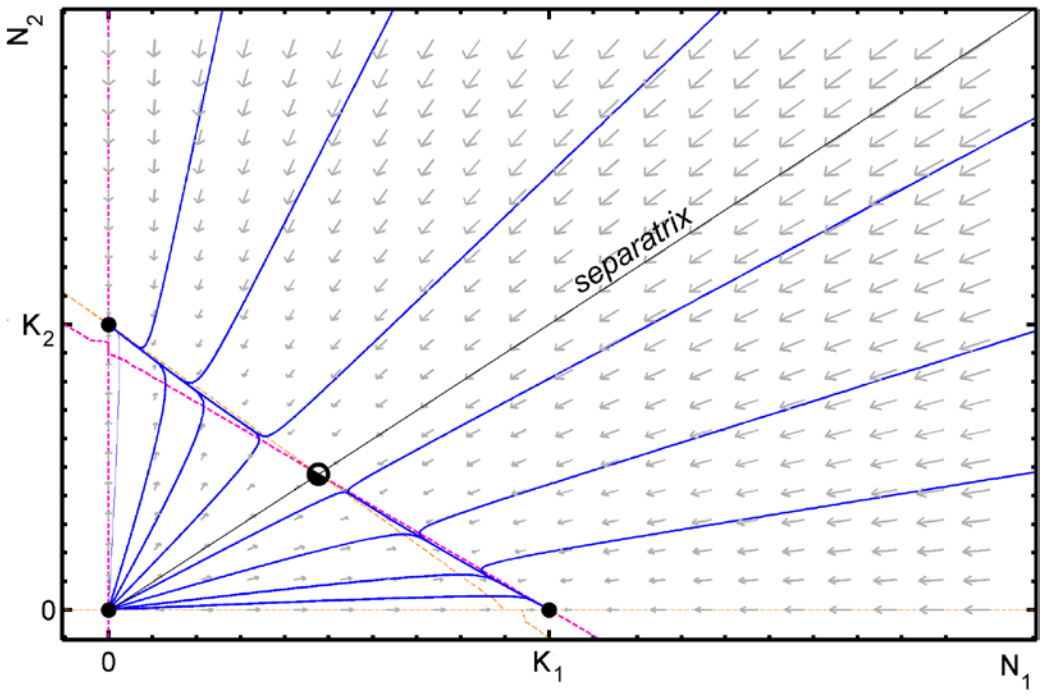


**Figure 3.5.** Phase plane portrait of Lotka-Volterra competition model, described by Eqs. (3.1) and (3.2), for $\alpha > \frac{K_1}{K_2}, \beta > \frac{K_2}{K_1}$, indicating bistability: either $N_1$ or $N_2$ will prevail.

A strong degree of competition is suggested by the case where $\alpha > \frac{K_1}{K_2}, \beta > \frac{K_2}{K_1}$ (Figure 3.5). The nullclines of $N_1$ and $N_2$ are represented by dashed pink and orange lines,

respectively. Their intersection marks the formation of a half-stable saddle point (recall Figure 1.6) at $(N_1^*, N_2^*) = \left(\frac{K_1 - \alpha K_2}{1-\alpha\beta}, \frac{K_2 - \beta K_1}{1-\alpha\beta}\right)$, which is graphically represented as a half-filled dot.

The resulting behaviors are described as *bistable* because the trajectories may converge to two possible equilibrium points given the same parameter values. Viewing the phase portrait, we observe that either species may prevail as the "winning" monoculture, while the "loser" species is driven to extinction. The initial conditions determine which equilibrium point will be approached by population trajectories. The line dividing the two locally stable regions is called the *separatrix* (Pastor, 2008). The trajectories divided by this line converge locally to the nearest stable boundary equilibrium, namely either $(K_1, 0)$ or $(0, K_2)$.

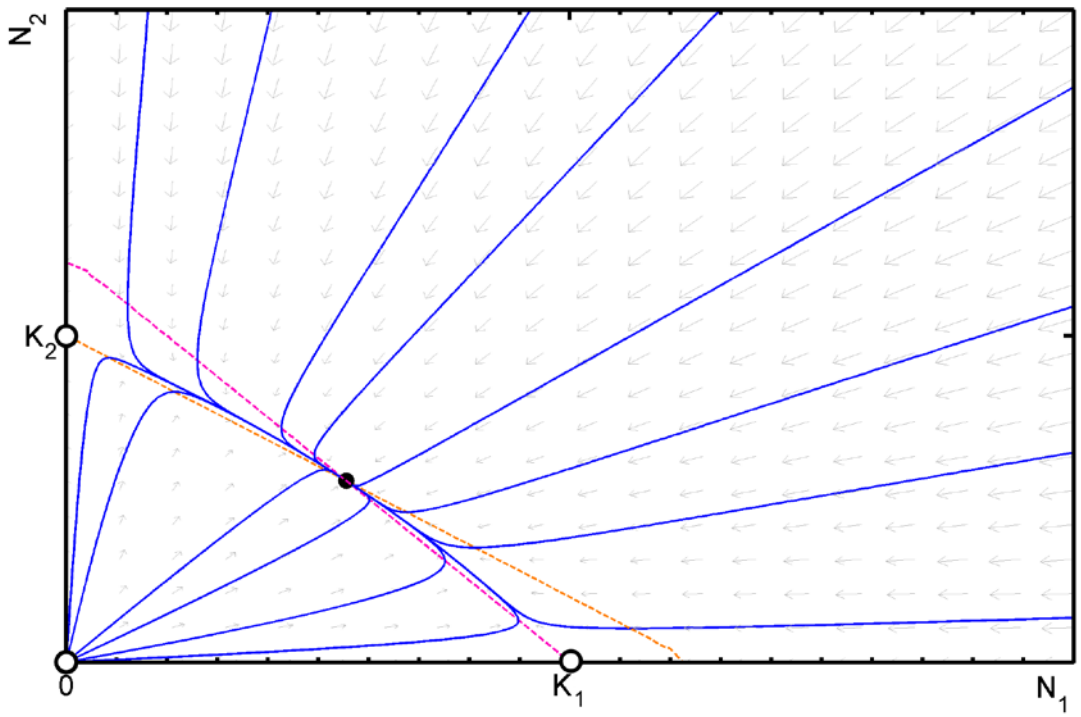


**Figure 3.6.** Phase plane portrait of Lotka-Volterra competition model, described by Eqs. (3.1) and (3.2), for $\alpha < \frac{K_1}{K_2}, \beta < \frac{K_2}{K_1}$, indicating coexistence.

Under conditions of *weak* competition, as depicted in Figure 3.6, both competition coefficients are low, such that $\alpha < \frac{K_1}{K_2}, \beta < \frac{K_2}{K_1}$, and as a result, both populations exist at a stable equilibrium. Thus, for stable coexistence to occur, interspecific competition coefficients must remain below the intraspecific competition thresholds (i.e., carrying capacities), which are imposed regardless of the presence or absence of the other species.

One might interpret this result, *prima facie*, in conflict with Gause's principle of competitive exclusion. Because, however, interspecific competition levels are weak (in fact, weaker than those for intraspecific competition), it can be concluded that the two species do not compete to a high enough degree for them to be considered true competitors. Thus, they are said to inhabit independent ecological niches, and Gause's principle is contested (Hardin, 1960).

***Local Linearization***

While our geometrical analysis appears sensible, let us verify the results of our model by linearizing it about the system's equilibria. Near equilibrium points, the dynamics of the system may be approximated by

$$\frac{du}{dt} = Au + Bv, \tag{3.18}$$

$$\frac{dv}{dt} = Cu + Dv, \tag{3.19}$$

where $u = N_1 - N_1^*$ and $v = N_2 - N_2^*$. At equilibrium, the associated Jacobian matrix, or *community matrix*, is given by

$$\mathbf{J}^* = \left[\begin{array}{cc} \frac{\partial f}{\partial N_1} & \frac{\partial f}{\partial N_2} \\ \frac{\partial g}{\partial N_1} & \frac{\partial g}{\partial N_2} \end{array}\right]\Bigg|_{N_1^*, N_2^*} = \left[\begin{array}{cc} \frac{r_1\left(K_1 - 2N_1^* - \alpha N_2^*\right)}{K_1} & \frac{-r_1\alpha N_1^*}{K_1} \\ \frac{-r_2\beta N_2^*}{K_2} & \frac{r_2\left(K_2 - 2N_2^* - \beta N_1^*\right)}{K_2} \end{array}\right]. \quad (3.20)$$

We can see that in the specific case of coexistence, the Jacobian is written

$$\mathbf{J}^*\Big|_{\text{coexistence}} = \left[\begin{array}{cc} \frac{r_1(K_1 - \alpha K_2)}{K_1(\alpha\beta - 1)} & -\frac{r_1\alpha(K_1 - \beta K_2)}{K_1(\alpha\beta - 1)} \\ -\frac{r_2\alpha(K_2 - \alpha K_1)}{K_2(\alpha\beta - 1)} & \frac{r_2(K_2 - \beta K_1)}{K_2(\alpha\beta - 1)} \end{array}\right]. \quad (3.21)$$

The condition for stability of coexistence requires that $\text{tr}(\mathbf{J})^* < 0$ and $\det(\mathbf{J})^* > 0$. We know that the trace is negative if $\alpha, \beta < \frac{K_{1,2}}{K_{1,2}}$, and that the determinant is positive if $\alpha\beta < 1$. Therefore, the product of the *intra*specific density-dependence coefficients is greater than those of *inter*specificity. The biological relevance of this reflects Gause's observations discussed prior, namely that "complete competitors cannot coexist" (Britton, 2003).

## 3.2 FACULTATIVE MUTUALISM MODEL

Facultative mutualism is a condition in which both species benefit from their mutual association. It is distinguished from *obligate* mutualism to the extent that facultative species may survive in the absence of each other, and obligate species will perish in the absence of one another.

An interesting example of facultative mutualism is found in the case of the Boran people of Kenya, who, in search of honey, use the guidance of a bird called the greater honeyguide (*Indicator indicator*) to locate colonies of honeybees. In doing so, a mutual benefit is granted to both species: the people receive food subsistence from the honey, and the bird receives the increased ability to feed on honeybee larvae and hive wax. Isack & Reyer's (1989) statistical analysis reveals significant correlations between each species' interspecific communications as well as the increased mutual success in locating the honeybee hives.

In reality, mutualisms are not necessarily, or often, symmetrical. For instance, the fitness of species $S_1$ may depend wholly on $S_2$, while the fitness of $S_2$ may depend only slightly on $S_1$. This relation would be called an obligate-facultative mutualism. For the sake of brevity, we will only be considering symmetrical associations (i.e., facultative-facultative and obligate-obligate).

We will approach the problem in a similar fashion as the Lotka-Volterra competition model by first assuming two species with populations $N_1$ and $N_2$ that grow logistically in each other's absence. Changing the sign of the interaction coefficients $\alpha$ and $\beta$ from

negative to positive, we obtain interaction terms that enhance growth rates rather than inhibit them. The adjusted equations governing mutual benefaction are denoted

$$\frac{dN_1}{dt} = r_1 N_1 \left[ 1 - \frac{(N_1 - \alpha N_2)}{K_1} \right], \tag{3.22}$$

$$\frac{dN_2}{dt} = r_2 N_2 \left[ 1 - \frac{(N_2 - \beta N_1)}{K_2} \right], \tag{3.23}$$

where $\alpha$ and $\beta$ clump many mechanisms together into phenomenological entities, which determine the strength of mutualistic benefaction from each species.

In the case of facultative mutualism, we set parameters $r_1$, $r_2$, $K_1$, $K_2$ to positive quantities, so that for a species in absence of its mutualist, the equilibrium population density will be equivalent to its carrying capacity $K_i$, $i = 1, 2$. That is to say, $N_1$ will grow towards its carrying capacity $K_1$ even in the absence of $N_2$, and *vice versa*.

### *Obtaining Equilibrium Points*

We obtain the system's equilibrium points by finding values of $N_1$ and $N_2$ for which $\frac{dN_1}{dt} = \frac{dN_2}{dt} = 0$ is satisfied. The following equilibrium points are obtained:

$$N_1^* = 0,\ N_2^* = 0 \tag{3.24}$$

$$N_1^* = K_1, N_2^* = 0 \tag{3.25}$$

$$N_1^* = 0,\ N_2^* = K_2 \tag{3.26}$$

$$N_1^* = \frac{-K_1 - \alpha K_2}{\alpha\beta - 1},\ N_2^* = \frac{-K_2 - \beta K_1}{\alpha\beta - 1} \tag{3.27}$$

We note that these equilibrium solutions bear a strong resemblance to those of the competition model, except for the change of signs of the critical point for coexistence.

***Geometrical Analysis***

The $N_1$ nullclines ($\frac{dN_1}{dt} = 0$) are given by the equations

$$N_1 = 0, \tag{3.28}$$

$$N_1 = K_1 + \alpha N_2, \tag{3.29}$$

and the $N_2$ nullclines ($\frac{dN_2}{dt} = 0$) are given by

$$N_2 = 0, \tag{3.30}$$

$$N_2 = K_2 + \beta N_1. \tag{3.31}$$

The dynamics of facultative mutualism differ between a weak case, where $\alpha\beta < 1$, and strong case, where $\alpha\beta > 1$. Nullclines intersect if $\alpha\beta < 1$, and they diverge if $\alpha\beta > 1$. Therefore, the only case in which a critical point occurs is the weak case. A stable node forms in the first quadrant where both nullclines cross, denoting stable coexistence (Figure 3.7); however, if nullclines diverge, then they do not cross at any point and the populations undergo unbounded growth (Figure 3.8), in what Robert May has called "an orgy of mutual benefaction" (1981).

The case of unbounded growth driven by positive feedback between both mutualists is not a realistic scenario. Some researchers have modified the problem such that limits are imposed on the mechanism of mutual positive feedback. For instance, Wolin and Lawlor (1984) consider the impact of mutualism with respect to recipient density via six different models: one model with per capita benefits of mutualism independent of recipient density, three models with mutualism effects most pronounced at a high density of recipients, and two models with mutualism effects most pronounced at a low density of recipients. The latter two 'low-density' models were unique in the sense that they always produced a

stable equilibrium, even in cases of *strong* facultative mutualism; that is to say, where interaction coefficients were $\alpha > \frac{K_1}{K_2}, \beta > \frac{K_2}{K_1}$ (1984).

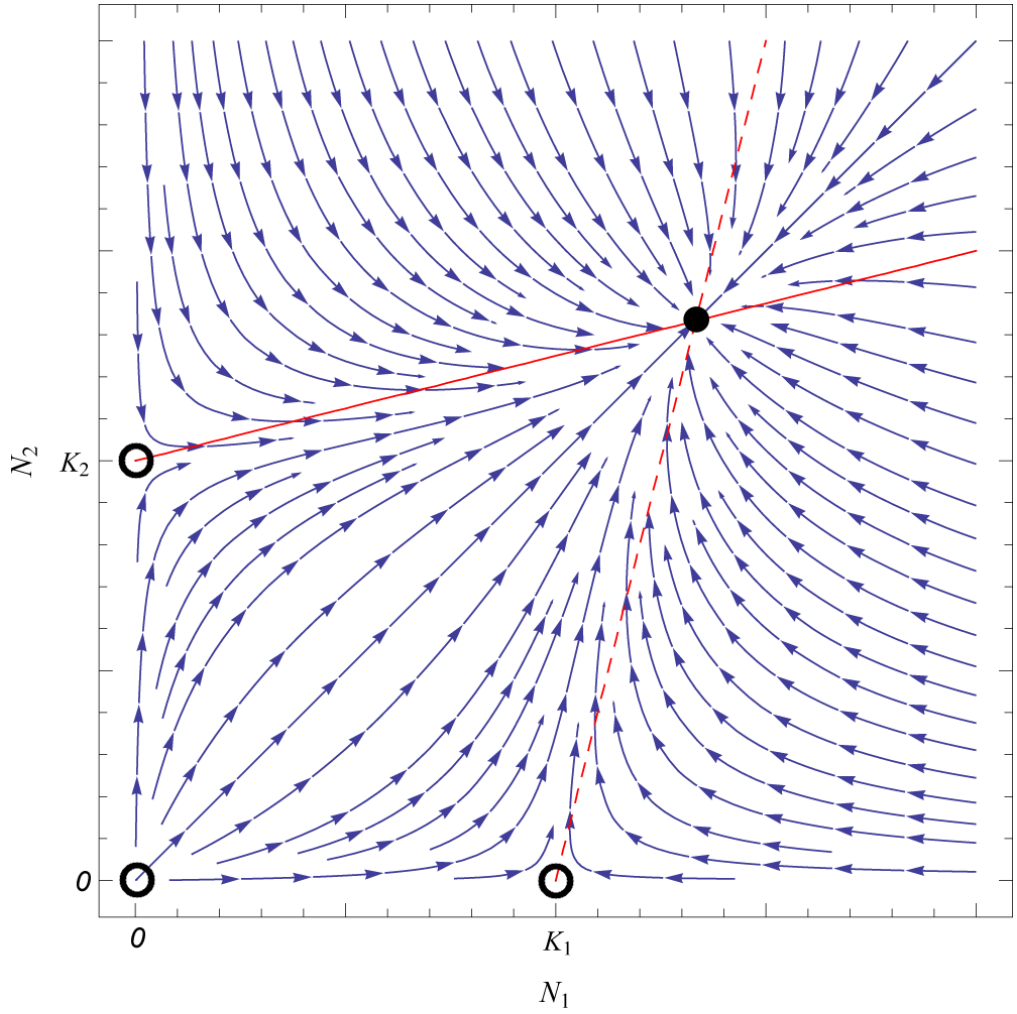


**Figure 3.7.** Phase plane portrait of Lotka-Volterra *weak* facultative mutualism, described by Eqs. (3.1) and (3.2), with $\alpha\beta < 1$.

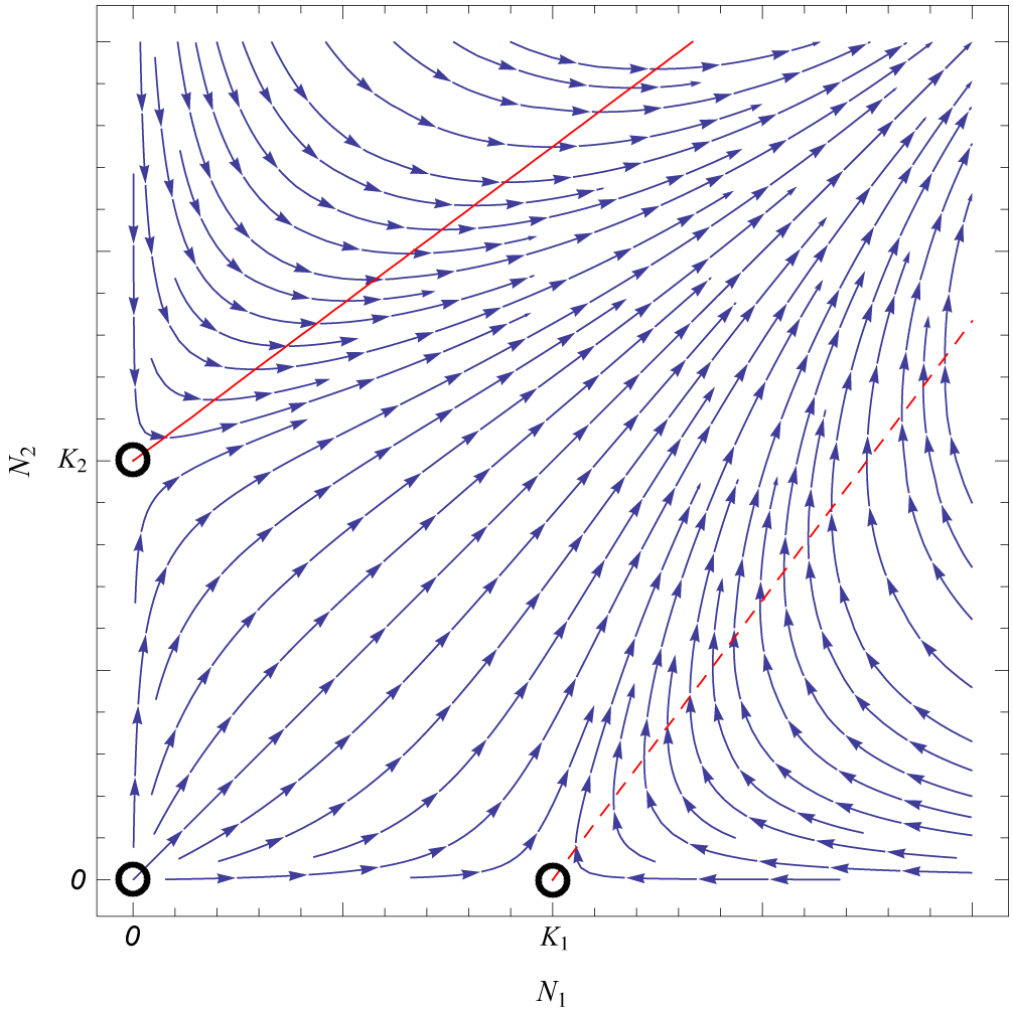


**Figure 3.8.** Phase plane portrait of the Lotka-Volterra *strong* facultative mutualism, described by Eqs. (3.1) and (3.2), with $\alpha\beta > 1$.

### *Local Linearization*

Given that coexistence occurs only in the *weak* case of facultative mutualism, we may begin our analysis evaluating the stable critical point that occurs when $\alpha\beta < 1$. The Jacobian matrix mirrors that of the competition model, except for the reversal of signs within the numerators:

$$\mathbf{J}^*\Big|_{\text{coexistence}} = \begin{bmatrix} \dfrac{r_1(K_1+\alpha K_2)}{K_1(\alpha\beta-1)} & -\dfrac{r_1\alpha(K_1+\beta K_2)}{K_1(\alpha\beta-1)} \\ -\dfrac{r_2\alpha(K_2+\alpha K_1)}{K_2(\alpha\beta-1)} & \dfrac{r_2(K_2+\beta K_1)}{K_2(\alpha\beta-1)} \end{bmatrix}. \tag{3.32}$$

We find the trace and determinant of $\mathbf{J}^*$ by

$$\text{tr}(\mathbf{J}^*) = \frac{(r_1+r_2)K_1K_2 + r_1\alpha K_2^2 + r_2\beta K_1^2}{K_1K_2(\alpha\beta-1)}, \tag{3.33}$$

$$\det(\mathbf{J}^*) = \frac{-r_1r_2(K_1+\alpha K_2)(K_2+\beta K_1)}{K_1K_2(\alpha\beta-1)}. \tag{3.34}$$

If $\text{tr}(\mathbf{J}^*) < 0$ and $\det(\mathbf{J}^*) > 0$, then the system is stable. Examining the case for weak facultative mutualism where $\alpha\beta < 1$, we find that, indeed, $\text{tr}(\mathbf{J}^*) < 0$ and $\det(\mathbf{J}^*) > 0$, indicating that the critical point is a stable node given the real, negative eigenvalues (Figure 3.7). Therefore, coexistence is guaranteed for the case of weak facultative mutualism, but not for strong facultative mutualism.

## 3.3 OBLIGATE MUTUALISM MODEL

In the case of obligate mutualism, we may use the same equations that were used for facultative mutualism: (3.22) and (3.23), except that the sign of parameters $r_1$, $r_2$, $K_1$, $K_2$ is reversed from positive to negative. Changing the carrying capacities may appear counterintuitive; however, it simply requires that neither species can survive in the absence of the other. Therefore both species are said to be obligate mutualists.

Obligate mutualism is exemplified by numerous species that rely on intracellular bacterial symbionts. These *endosymbionts*, in turn, rely on their hosts for survival and fecundity. The results of Wernegreen's (2002) genomic analysis of two obligate mutualists (*B. aphidicola* of aphids and *W. glossinidia* of tsetse flies) reveal marked gene loss and an integration of metabolic function between endosymbiont and host. In a similar vein, the integration of functional biological machinery arises in *endosymbiotic theory*, pioneered by Lynn Margulis, wherein the endosymbiotic union of bacteria is held to be responsible for the origins of mitochondria and chloroplasts in eukaryotic cells (Kozo-Polyansky, 2010).

Using the same equations as in the prior case of facultative mutualism to define the $N_1$ and $N_2$ nullclines, namely Eqs. (3.28) through (3.31), we should note the changes that occur due to $K_1$ and $K_2$ becoming negative quantities, namely that both species become reliant on each other for survival.

### *Geometrical Analysis*

In the case where $\alpha\beta < 1,$ the nullclines of $N_1$ and $N_2$ do not intersect in the first quadrant, and the stable node at $(0,0)$ is the only equilibrium, so both populations decay

towards extinction (Figure 3.9). In this case, the two species' interdependent relations are too weak for either species to benefit the other to the point of survival. The probability of a *weak* obligate relationship occurring in nature would be rare since the two species are wholly interdependent.

Conversely, when $\alpha\beta > 1$, a saddle point forms at the point of intersection between the two nullclines (Figure 3.10). Here, if densities of mutualists are below the saddle point threshold, then both populations decay towards extinction despite the strong nature of their interaction. If mutualist densities are sufficiently high, once more, both populations engage in an "orgy of mutual benefaction," where orbits diverge to infinity.

These results indicate that coexistence between mutualistic species in the Lotka-Volterra models, whether facultative-facultative or obligate-obligate, is possibly only if interspecific interactions are sufficiently weak. Pastor (2008) speculates that strong interspecies interactions appear to destabilize food webs. Additionally, the absence of complex eigenvalues of the Jacobian matrices prohibits the possibility of stable limit cycles from occurring.

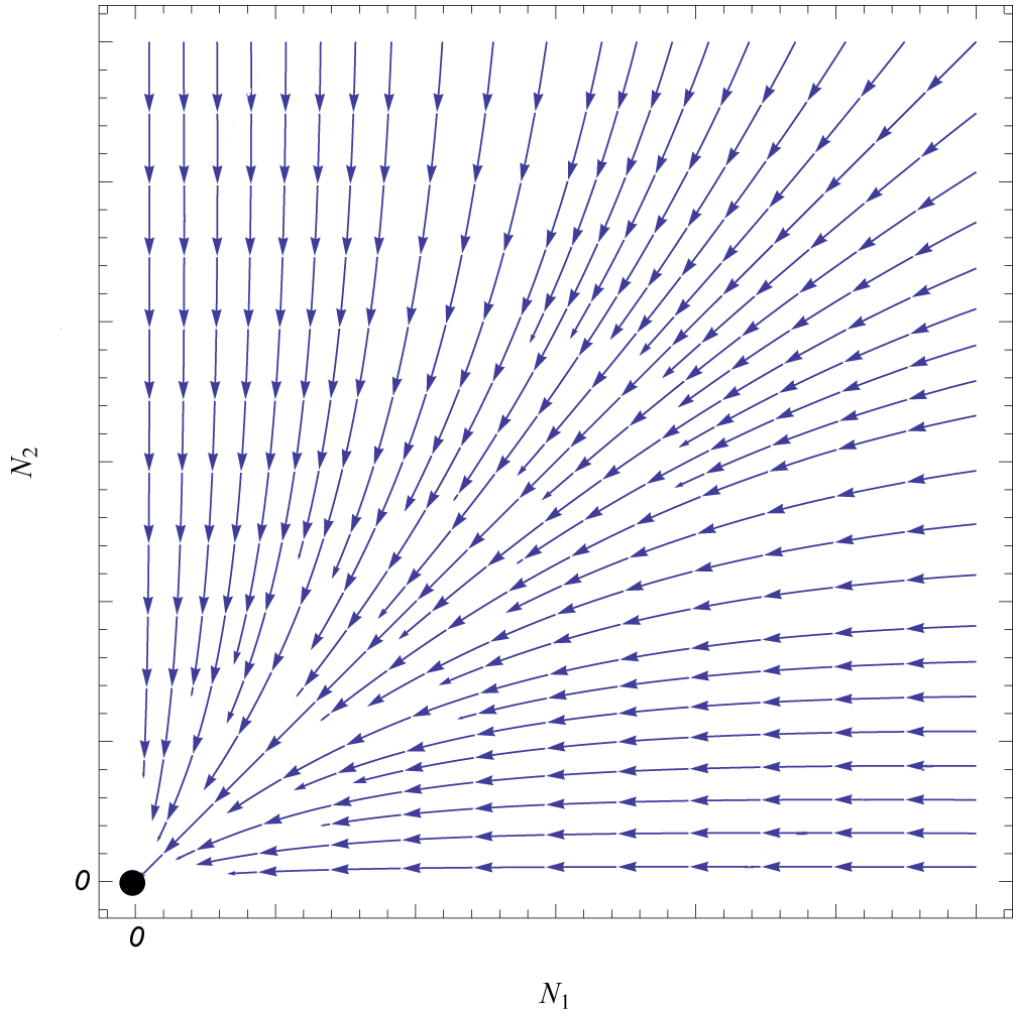


**Figure 3.9.** Phase plane portrait of the Lotka-Volterra *weak* obligate mutualism model, described by Eqs. (3.22) and (3.23), with $\alpha\beta < 1$.

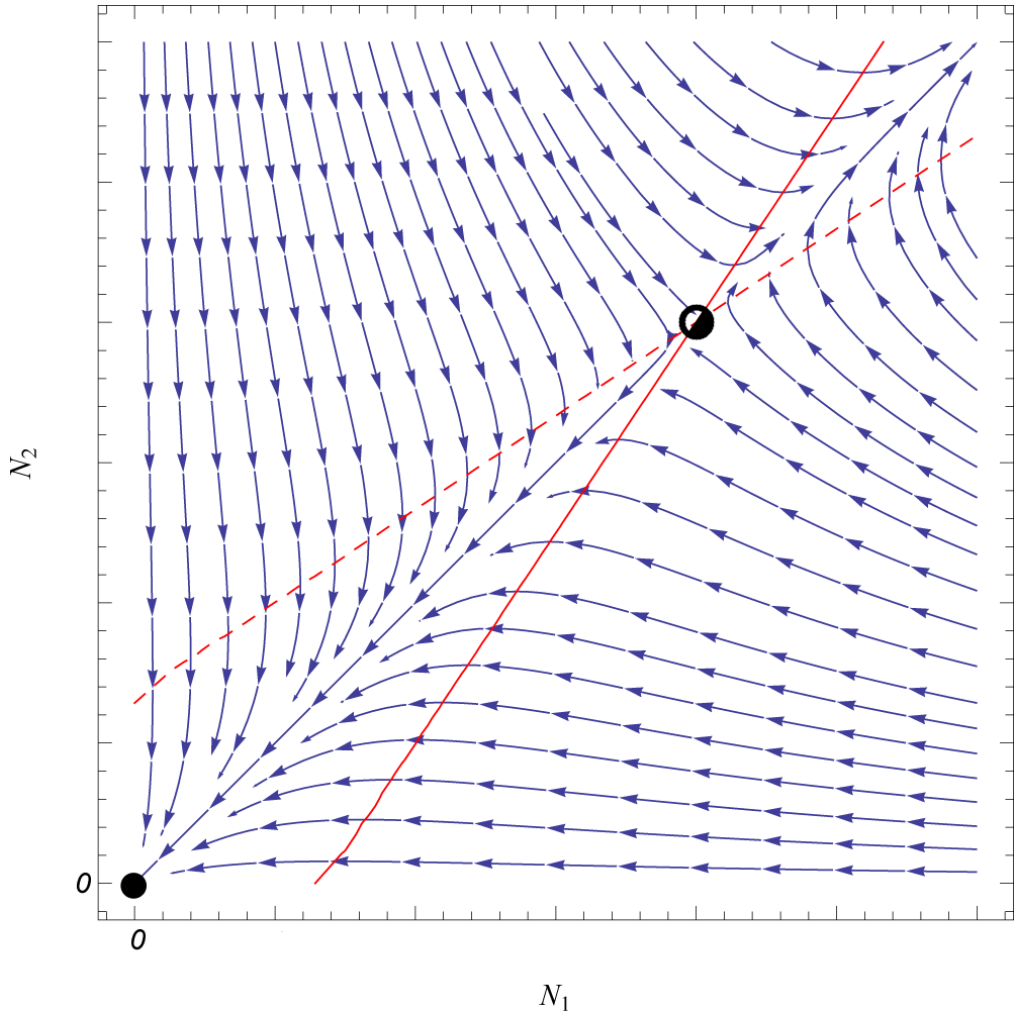


**Figure 3.10.** Phase plane portrait of the Lotka-Volterra *strong* obligate mutualism model, described by Eqs. (3.22) and (3.23), with $\alpha\beta > 1$.

## 3.4 PREDATOR-PREY MODEL

Recalling the phenomenological nature of the "carrying capacity" term $K$ of the logistic model, we found that $K$ therefore is independently derived, and has little to do with the actual surrounding environment. Here, we will begin by eliminating the phenomenological term $K$ for both species such that a "new" carrying capacity is determined, instead, from the interactions between both species (Pastor, 2008). Along these lines, it should be easy to determine whether the exponential growth of prey is stabilized by predation, and likewise whether the growth of predators is stabilized by the decline of their food source, prey.

Consider two populations, $N_1$ and $N_2$, which represent preys and a predators, respectively. The coupled system of equations of the Lotka-Volterra predator-prey model follows as

$$\frac{dN_1}{dt} = rN_1 - \beta N_1 N_2, \tag{3.35}$$

$$\frac{dN_2}{dt} = \gamma N_1 N_2 - \delta N_2, \tag{3.36}$$

where, in the equation of the prey population (3.35), $r$ is the Malthusian growth parameter and $\beta$ is an interaction coefficient determining the rate at which predation (i.e., prey death) may occur. The second term of (3.35) assumes that the product of both species' densities $N_1 N_2$ accounts for the fact that both species must meet in order for predation to occur, and the coefficient $\beta$ determines the probability of a predation event successfully occurring. In Eq. (3.36) of the predator population, $\gamma$ is the interaction coefficient determining the amount of biomass transferred from prey to predator for each successful predation event.

The constant $\delta$ serves as the predator death rate parameter, which mediates the constant exponential decay of predators.

The Lotka-Volterra predator-prey model can be further elucidated by outlining its assumptions. Prey growth proceeds exponentially without limit in the absence of predators, causing dynamics to proceed in a Malthusian fashion such that $\frac{dN_1}{dt} = rN_1,\ (r > 0)$. Predator growth is dependent on prey abundance, and therefore, if prey are absent then predator growth decays exponentially such that $\frac{dN_2}{dt} = -\delta N_2,\ (\delta > 0)$. The predation rate is dependent on the likelihood of a predator individual meeting a prey individual in a spatially homogeneous population distribution, providing the terms governing prey death and predator birth. That is to say, the predator growth rate is proportional to the number of prey present ($\gamma N_1 N_2$, where $\gamma$ is a positive constant), and likewise, prey death is proportional to the number of predators present ($-\beta N_1 N_2$, where $\beta$ is a positive constant).

***Geometrical Analysis***

Initially, we may view the general behavior of $N_1$ and $N_2$ by plotting the $(N_1, N_2)$ vector field (Figure 3.11) and by determining the system's nullclines, which occur where $\frac{dN_1}{dt} = \frac{dN_2}{dt} = 0$. Following along the lines of Pastor (2008), we factor out $N_1$ and $N_2$ on the right-hand-side of each equation, yielding

$$\frac{dN_1}{dt} = N_1(r - \beta N_2), \tag{3.37}$$

$$\frac{dN_2}{dt} = N_2(\gamma N_1 - \delta). \tag{3.38}$$

The intersection of $N_1$ and $N_2$ reveals the system's point of equilibrium. Trivial nullclines are found at $N_1 = 0$ and $N_2 = 0$, with each axis representing the nullcline for the other species (Figure 3.11). Setting the terms in parentheses of Eqs. (3.37) and (3.38) equal to zero such that

$$r - \beta N_2 = 0, \tag{3.39}$$

$$\gamma N_1 - \delta = 0, \tag{3.40}$$

we achieve nullclines for $N_1$ and $N_2$. For $N_1$, we get the nullcline $N_2 = \frac{r}{\beta}$, and for $N_2$, we get $N_1 = \frac{\delta}{\gamma}$ (Figure 3.11). Notice that the nullcline for each species is dependent on the values of the other species as opposed to its own population density.

Alternatively, the net dynamics of the model can be viewed in Figure 3.12, which confirms the steady oscillatory behavior, suggested initially by the vector field (Figure 3.11). When $N_2 < \frac{r}{\beta}$, the decline of the prey population is less than its growth rate, and thus the prey population increases: $\left(\frac{dN_1}{dt} > 0\right)$. Likewise, when $N_2 > \frac{r}{\beta}$, the predation upon prey by predators dominates the prey growth factor, and therefore the prey population decreases: $\left(\frac{dN_1}{dt} < 0\right)$. The same mode of analysis can be performed for viewing predator dynamics. When $N_1 < \frac{\delta}{\gamma}$, the conversion of prey biomass into predator biomass by means of predation is outweighed by the constant mortality of predators; therefore, the predator population declines: $\left(\frac{dN_2}{dt} < 0\right)$, and when $N_1 > \frac{\delta}{\gamma}$, the growth of predators via predation outweighs the mortality of predators, and therefore, the predator population grows: $\left(\frac{dN_2}{dt} > 0\right)$.

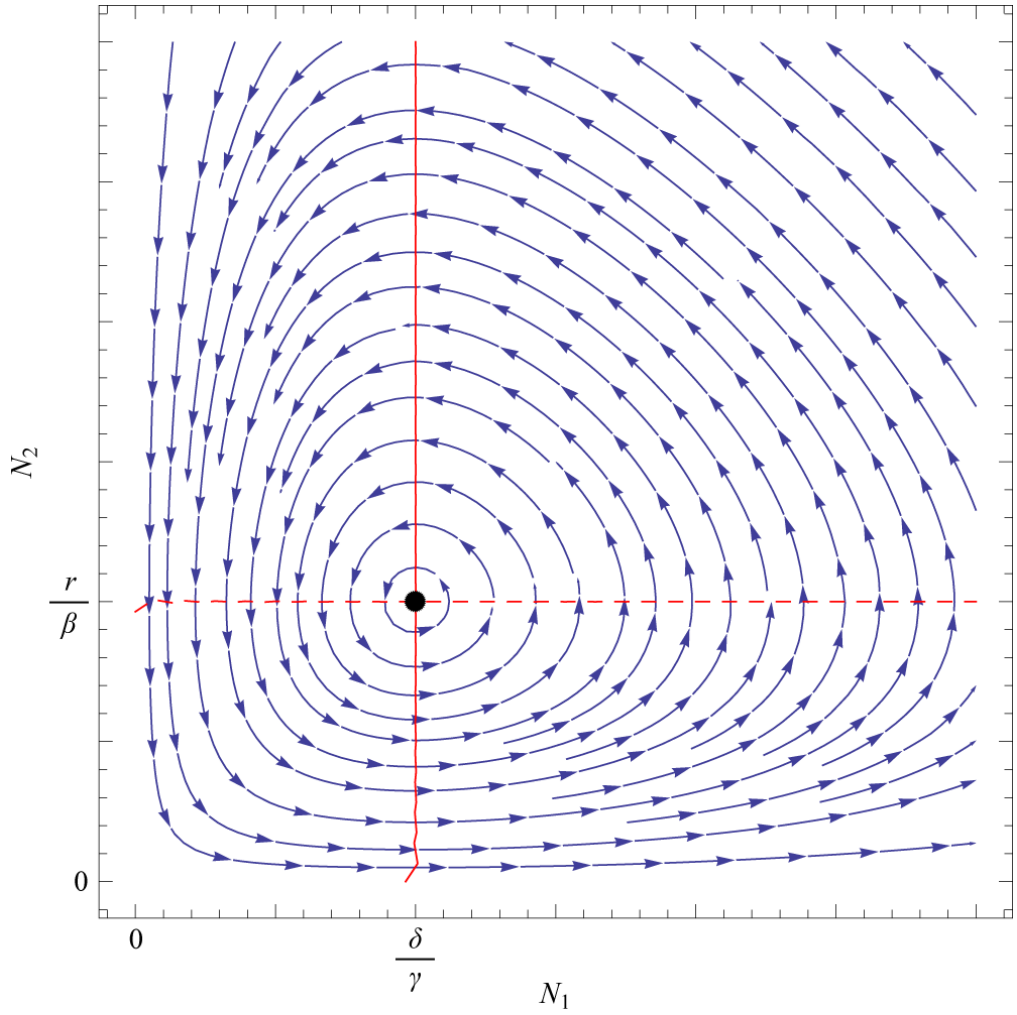


**Figure 3.11.** Phase plane portrait of Lotka-Volterra predator-prey system, described by Eqs. (3.35) and (3.36).

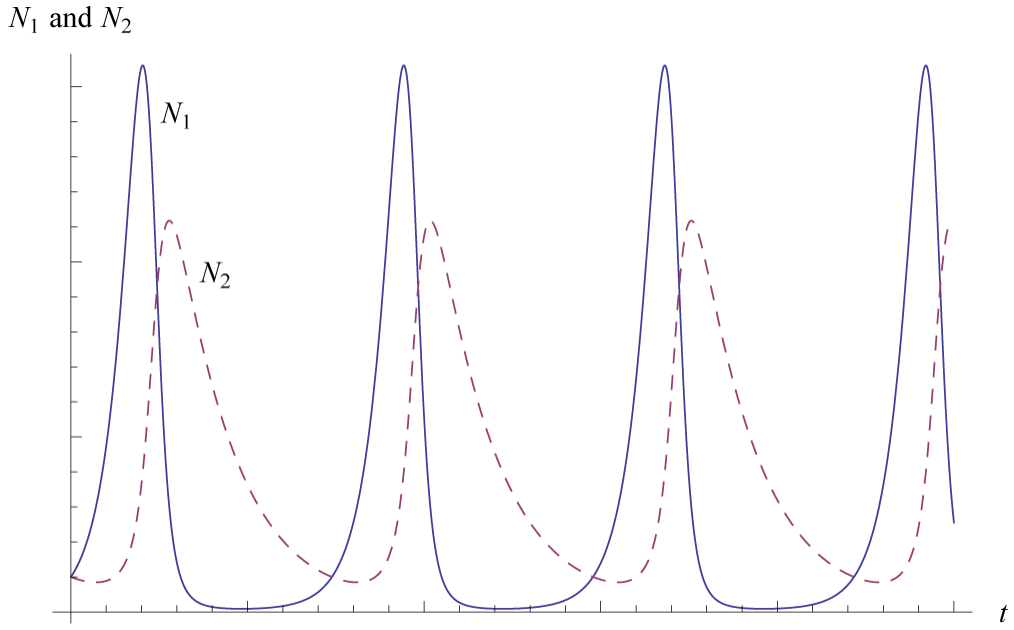


**Figure 3.12.** Dynamics of Lotka-Volterra predator-prey system, given by Eqs. (3.35) and (3.36).

***Local Linearization***

Setting both equations (3.35) and (3.36) equal to zero, and solving for $N_1$ and $N_2$, we yield the following equilibrium points:

$$N_1^* = 0,\ N_2^* = 0 \tag{3.41}$$

and

$$N_1^* = \frac{\delta}{\gamma},\ N_2^* = \frac{r}{\beta}. \tag{3.42}$$

Near equilibrium points, the dynamics of the system may be approximated by

$$\frac{du}{dt} = Au + Bv, \tag{3.43}$$

$$\frac{dv}{dt} = Cu + Dv, \tag{3.44}$$

where $u = N_1 - N_1^*$ and $v = N_2 - N_2^*$. Constants are given by the community matrix

$$\mathbf{J}^* = \left[\begin{array}{cc} \frac{\partial f}{\partial N_1} & \frac{\partial f}{\partial N_2} \\ \frac{\partial g}{\partial N_1} & \frac{\partial g}{\partial N_2} \end{array}\right]_{(N_1^*, N_2^*)} = \begin{bmatrix} r - \beta N_2^* & -\beta N_1^* \\ \gamma N_2^* & \gamma N_1^* - \delta \end{bmatrix} \tag{3.45}$$

Evaluating the first equilibrium at the origin $(0,0)$, the Jacobian becomes

$$\mathbf{J}^*\big|_{(0,0)} = \begin{bmatrix} r & 0 \\ 0 & -\delta \end{bmatrix}. \tag{3.46}$$

The eigenvalues determine the stability of the point, and are found by

$$\lambda_{1,2} = \frac{r-\delta}{2} \pm \frac{\sqrt{(r+\delta)^2}}{2}, \tag{3.47}$$

$$\lambda_1 = r, \qquad \lambda_2 = -\delta. \tag{3.48}$$

In the Lotka-Volterra equations both $r, \delta > 0$; therefore, $\lambda_1 > 0$ and $\lambda_2 < 0$. Therefore, the equilibrium point at $(0,0)$ is a *saddle point* (recall Figures 1.5 and 1.6).

Evaluating the second equilibrium at coexistence $(\frac{\delta}{\gamma}, \frac{r}{\beta})$, the Jacobian becomes

$$\mathbf{J}^*\big|_{\text{coexistence}} = \begin{bmatrix} 0 & \frac{-\beta\delta}{\gamma} \\ \gamma r & 0 \end{bmatrix}. \tag{3.49}$$

The eigenvalues, therefore, of the equilibrium point at $N_1^* = \frac{\delta}{\gamma}$ and $N_2^* = \frac{r}{\beta}$ are given by

$$\lambda_{1,2} = \pm\sqrt{-r\delta}. \tag{3.50}$$

These are purely complex eigenvalues, which indicates that the equilibrium is a neutrally stable *center* (recall Figure 1.6).

# CHAPTER 4: CONCLUDING REMARKS

In Chapter 1 we provided an outline of general dynamical systems, modeling methodology, and the associated history of differential equations in modeling population dynamics. We discovered the multitude of uses that differential equations have served in modeling ecological dynamics, not to mention their ease of analysis and parsimonious assumptions. Beginning with the simplest one-dimensional models in Chapter 2, we carried out a gradual modification of each subsequent model and analyzed its behaviors and ecological consequences. In Chapter 3, we followed the same basic process for two-dimensional models. The basis of this progression has served to demonstrate how one might go about formulating a complex model from simple foundations in a piecemeal fashion.

The current state of affairs in ecological population modeling continues to find numerous uses for differential equations-based modeling. The bulk of ecological research, however, has become drastically refocused as the need to address global issues, from climate change to naturally-driven catastrophes, has become ever more prevalent. The classical approach of ecology, as Miao, et al. (2009) put it, "has shifted to a new era in which ecological science must play a greatly expanded role in improving the human condition by addressing the sustainability and resilience of socio-ecological systems." Temporal and spatial scales are expanded in these increasingly sophisticated global models, in turn availing longer-term and longer-range predictions (Miao, Carstenn, & Nungesser, 2009).

However, much like the unpredictability of weather patterns, most ecological systems are chaotic and, in turn, difficult to forecast.

Both the historical development of population dynamics (outlined in Section 1.4) and schematization of ecological modeling (Section 1.2) illuminate the progression towards globally-informed ecological modeling practices. The mathematical models considered throughout this work have focused primarily on small-scale systems containing relatively few processes, yet their principles are, to a large degree, generalizable to higher dimensions. Stochasticity and spatiality were ignored throughout this work; however, stochastic (i.e., probabilistic) techniques have become well-established, and there are numerous methods that account for spatial dynamics, including agent-based models such as cellular automata, or partial differential equations.

The most intense issues of global ecology include anthropogenic impacts on earth's ecosystems and climate (Yue, Jorgensen, & Larocque, 2010), and global health issues. Humanity's response to mitigating such impacts relies, to a large degree, on modeling.

The rapid changes sustained by human populations and their environment in recent times present an unprecedented demand for ecologists to forge new connections with planning, policy-making, and risk- and decision- analysis. For example, the MIDAS project, funded by the National Institute of Health, develops models intended for policymakers, public health workers, and other researchers interested in emerging infectious diseases. Environmental conservation policy- and decision-making also relies heavily on well-formulated models. The CREAM project funded by the European Union serves as one such example, having initiated over a dozen ecological modeling projects involving chemical risk assessment (Schmolke, Thorbek, DeAngelis, & Grimm, 2010). Additionally, a number of

intergovernmental panels share data and enact decision-making based on applications of ecological modeling; these include Man and the Biosphere (MAB), World Climate Research Program (WCRP), the Intergovernmental Panel on Climate Change (IPCC), International Geosphere-Biosphere Program (IGBP), International Human Dimensions Program on Global Environmental Change (IHDP), International Program of Biodiversity Science (DIVERSITAS), Millennium Ecosystem Assessment (MA), Earth System Science Partnership (ESSP), and Global Earth Observation System of Systems (GEOSS), among others (Yue, Jorgensen, & Larocque, 2010).

Classical infectious disease dynamics, including Kermack and McKendrick's "SIR" model (Section 1.4), rely on differential equations and have been praised for their maximal parsimony (Epstein, 2009). Such models, however, turn out to be poorly-suited to capturing the complex behaviors of global spread, and many investigators have opted instead for individual- or agent-based models (ABMs). These models are formulated from the bottom-up by individuals whose interactions and behaviors are governed by a set of rules. As Epstein writes, "agents can be made to behave something like real people: prone to error, bias, fear and other foibles" (2009). Thus, ABMs embrace the complexity of social networks and the interactions between individuals (2009), albeit at a heightened computational expense. Their utility is exemplified by virtue of the fact that they provide a base case (as opposed to 'crystal ball' forecast) of material scenarios. With the base case in hand, the model can be run repeatedly under varying circumstances to examine the effects of different environmental conditions and agent-based configurations (2009), thereby informing policy- and decision-making.

# REFERENCES


Bacaër, N. (2011). *A Short History of Mathematical Population Dynamics* (p. 160). London: Springer.

Berryman, A. A., & Kindlmann, P. (2008). *Population systems: a general introduction*. *Population (English Edition)* (p. 222). London: Springer-Verlag.

Britton, N. F. (2003). *Essential Mathematical Biology*. *Mathematical Medicine and Biology* (Vol. 20, p. 370). London: Springer.

Courchamp, F., Clutton-Brock, T., & Grenfell, B. (1999). Inverse density dependence and the Allee effect. *Trends in ecology & evolution (Personal edition)*, *14*(10), 405-410.

Courchamp, F., Luděk, B., & Gascoigne, J. (2008). *Allee Effects in Ecology and Conservation* (p. 256). Oxford: Oxford University Press.

Edelstein-Keshet, L. (2005). *Mathematical Models in Biology* (p. 586). Philadelphia, PA: SIAM.

Epstein, J. M. (2009). Modelling to contain pandemics. *Nature*, *460*(7256), 687.

Gause, G. F. (1932). Experimental studies on the struggle for existence. *Journal of Experimental Biology*, *9*, 389–402.

Gause, G. F. (1934). *The Struggle for Existence*. Baltimore, MD: Williams & Wilkins.

Gilpin, M. E., & Ayala, F. J. (1973). Global models of growth and competition. *Proceedings of the National Academy of Sciences of the United States of America*, *70*(12), 3590-3.

Hardin, G. (1960). The Competitive Exclusion Principle. *Science*, *131*(3409), 1292-1297.

Howard, L. O., & Fiske, W. F. (1911). *Importation into the U.S. of the Parasites of the Gipsy Moth and the Browntail Moth* (p. 311).

Isack, H. A., & Reyer, H.-U. (1989). Honeyguides and honey gatherers: interspecific communication in a symbiotic relationship. *Science*, *243*(4896), 1343–1343. American

Association for the Advancement of Science, 1333 H St, NW, 8 th Floor, Washington, DC, 20005, USA.

Jennings, H. S. (1942). Biographical Memoir of Raymond Pearl (1879-1940). *National Academy of Sciences of the United States of America Biographical Memoirs* (Vol. 31, pp. 293-348).

Kaplan, D., & Glass, L. (1995). *Understanding Nonlinear Dynamics* (p. 440). New York, NY: Springer.

Kermack, W. O., & McKendrick, A. G. (1927). A Contribution to the Mathematical Theory of Epidemics. *Proceedings of the Royal Society of London. Series A, Containing Papers of a Mathematical and Physical Character*, *115*(772), 700-721. The Royal Society.

Kingsland, S. E. (1985). *Modeling nature: Episodes in the history of population ecology* (p. 267). Chicago: University of Chicago Press.

Kot, M. (2001). *Elements of Mathematical Ecology* (p. 447). Cambridge: Cambridge University Press.

Kozo-Polyansky, B. M. (2010). *Symbiogenesis: a new principle of evolution*. (V. Fet & L. Margulis, Eds.)*Theory in biosciences = Theorie in den Biowissenschaften* (Vol. 128, p. 240). Cambridge, MA: Harvard University Press.

Lorenz, E. N. (1963). Deterministic Nonperiodic Flow1. *Journal of the Atmospheric Sciences*, *20*(2), 130-141.

Lotka, A. J. (1907). Relation between birth rates and death rates. *Science*, *26*(653), 21-22.

Lotka, A. J. (1920). Analytical note on certain rhythmic relations in organic systems. *Proceedings of the National Academy of Sciences of the United States of America*, *6*(7), 410-415. National Academy of Sciences.

MacArthur, R., & Wilson, E. O. (1967). *The Theory of Island Biogeography* (p. 203). Princeton, NJ: Princeton University Press.

MacArthur, Robert, & Levins, R. (1967). The Limiting Similarity, Convergence, and Divergence of Coexisting Species. *The American Naturalist*, *101*(921), 377-385. The University of Chicago Press for The American Society of Naturalists.

Malthus, T. (1798). *An Essay on the Principle of Population, as it Affects the Future Improvement of Society with Remarks on the Speculations of Mr. Godwin, M. Condorcet, and Other Writers* (Vol. 6, p. 340). London.

May, R. M. (1981). *Theoretical Ecology: principles and applications* (2nd ed., p. 489). Oxford: Wiley-Blackwell.

May, R. M. (2001). *Stability and complexity in model ecosystems* (p. 235). Princeton University Press.

Maynard Smith, J. (1974). *Models in Ecology* (p. 146). Cambridge: Cambridge University Press.

Meszéna, G., Gyllenberg, M., Pásztor, L., & Metz, J. a J. (2006). Competitive exclusion and limiting similarity: a unified theory. *Theoretical population biology*, *69*(1), 68-87.

Miao, S., Carstenn, S., & Nungesser, M. (Eds.). (2009). *Real World Ecology: Large-Scale and Long-Term Case Studies and Methods* (p. 303). New York, NY: Springer.

Murray, J. (2002). *Mathematical Biology: An Introduction, Volume 1* (3rd ed., p. 551). New York, NY: Springer.

Pastor, J. (2008). *Mathematical Ecology of Populations and Ecosystems*. *Ecosystems* (p. 319). Oxford: Wiley-Blackwell.

Pearl, R. (1999). The Raymond Pearl Collection. *The Alan Mason Chesney Medical Archives of The Johns Hopkins Medical Institutions*. Retrieved January 5, 2011, from http://www.medicalarchives.jhmi.edu/sgml/pearl.html.

Pearl, R., Miner, J. R., & Parker, S. L. (1927). Experimental Studies on the Duration of Life. XI. Density of Population and Life Duration in Drosophila. *The American Naturalist*, *61*(675), 289-318. The University of Chicago Press for The American Society of Naturalists.

Pearl, R., & Reed, L. J. (1920). On the Rate of Growth of the Population of the United States Since 1790 and its Mathematical Representation. *Proceedings of the National Academy of Sciences*, *6*(6), 275-288.

Popper, K. R. (1992). *The logic of scientific discovery*. *New Yorker, The* (p. 513). New York, NY: Routledge.

Schmolke, A., Thorbek, P., DeAngelis, D. L., & Grimm, V. (2010). Ecological models supporting environmental decision making: a strategy for the future. *Trends in Ecology & Evolution*, *25*, 479-486. Retrieved from http://linkinghub.elsevier.com/retrieve/pii/S016953471000100X.

Schoener, T. W. (1986). Mechanistic Approaches to Community Ecology: A New Reductionism? *American Zoologist*, *26*(1), 81-106. Oxford University Press.

Sibly, R. M., Barker, D., Denham, M. C., Hone, J., & Pagel, M. (2005). On the regulation of populations of mammals, birds, fish, and insects. *Science*, *309*(5734), 607-10.

Sigler, L. E. (2002). *Fibonacci's Liber Abaci*. London: Springer-Verlag.

Strogatz, S. H. (1994). *Nonlinear Dynamics and Chaos: With Applications to Physics, Biology, Chemistry, and Engineering* (p. 498). Reading, MA: Perseus Books.

Verhulst, P.-F. (1845). Recherches mathématiques sur la loi d'accroissement de la population. *Nouv. mém. de l'Academie Royale des Sci. et Belles-Lettres de Bruxelles*, *18*, 1-41.

Wernegreen, J. J. (2002). Genome evolution in bacterial endosymbionts of insects. *Nature reviews. Genetics*, *3*(11), 850-61.

Wolin, C. L., & Lawlor, L. R. (1984). Models of facultative mutualism: density effects. *American Naturalist*, *124*(6), 843–862. JSTOR.

Yue, T.-X., Jorgensen, S. E., & Larocque, G. R. (2010). Progress in global ecological modelling. *Ecological Modelling*. Elsevier B.V.